Adaptive Decision-Feedback Multiuser Detection for DS-CDMA Systems

Min Li

A Thesis

in

The Department

of

Electrical and Computer Engineering

Presented in Partial Fulfillment of the Requirements

for the Degree of Master of Applied Science

Concordia University

Montreal, Quebec, Canada

November 2004

Your file Votre référence
ISBN: 0-494-04382-2
Our file Notre référence
ISBN: 0-494-04382-2

Abstract

Adaptive Decision-Feedback Multiuser Detection for DS-CDMA Systems

Min Li

Multiuser detection (MUD) has been proposed as a way to combat multiple access interference (MAI) in direct-sequence code-division multiple-access (DS-CDMA) systems. The optimum multiuser detector has a high computational complexity. For that reason, the research for MUD techniques which successfully negotiate the trade-off between performance and complexity becomes increasingly important.

In this thesis, we propose a modified multistage linear parallel interference cancellation (PIC) structure using the blind adaptive minimum mean-output-energy (MMOE) algorithm for DS-CDMA systems. The proposed receiver has a computational complexity that is linear in the number of users, and exhibits a performance close to the optimum linear minimum mean-squared-error (LMMSE) receiver whose complexity has a cubic dependence on the number of users. Moreover, the proposed blind adaptive MMOE-PIC receiver requires no side information on users' received signal amplitudes, which can further lower the complexity of the overall system.

Another multistage detector with low complexity is introduced for DS-CDMA

systems over both flat and frequency-selective fading channels. The proposed detector employs the blind adaptive multiuser receiver as the first stage followed by stages with interference cancellation (IC). The performance of the proposed detector is very close to the single user bound and is independent of system loads in flat fading channels. In multipath fading channels, from low to moderate SNR's, the proposed receiver suffers less than 1dB penalty compared with ideal detection without interference. At high SNR's, an error floor occurs for high loaded systems.

Finally we consider a class of decision-feedback detectors (DFDs) based on the modified MMSE performance criterion in the presence of dynamic fading. Successive cancellation is employed to mitigate the effects of error propagation. To equalize the performance over the users with successive cancellation, an iterative DFD is presented, which consists of cascaded DFDs, each performing successive cancellation. The effect of error propagation is illustrated through simulation. Although error propagation can significantly degrade performance, the proposed DFDs still offer a significant performance and capacity gains relative to the modified LMMSE detector in fading channels.

Acknowledgements

I would like to acknowledge appreciation to a number of people who have contributed directly or indirectly to the writing of this dissertation.

I am so fortunate to have the opportunity to work on this interesting topic under the supervision of Dr. Walaa A. Hamouda. I want to express my sincere gratitude to him and truly appreciate his constructive guidance, valuable advice, editing of this manuscript and financial support.

My great thanks must go to my parents who did everything they could to educate me with all the difficulties they had.

Finally, I want to thank all my friends who help and encourage me throughout my study in Concordia University.

To my parents and brother

Contents

List of Figures

List of Tables

Chapter 1

Introduction

1.1 DS-CDMA Communications

Over the last decade the interest in wireless communications has dramatically increased. Existing forms of wireless communications: cellular mobile phones, wireless networks, cordless phones and radio pages, continue to experience explosive growth, and show a large increase in the number of users. Capacity, radio spectrum utilization efficiency and service quality are of primary concern, but also other factors such as the system complexity and the associated cost are of great concern [1]. Digital modulation, detection and multiple access techniques are essential components in the design of any communication system. During last decade, many known techniques have been analyzed and re-evaluated for the mobile communications. Spread-spectrum communications is a well-known technique which has found a place in cellular mobile systems. In particular, DS-CDMA systems have attracted much interest.

Code-division multiple-access is one of several methods of multiplexing wireless users. In CDMA, users are multiplexed by distinct codes rather than by orthogonal frequency bands, as in frequency-division multiple-access (FDMA), or by orthogonal time slots, as in time-division multiple-access (TDMA). In CDMA, all users can transmit at the same time. Also, each user is allocated the entire available frequency spectrum for transmission. Hence, CDMA is also known as spread-spectrum multiple-access (SSMA), or simply spread-spectrum communications.

CDMA has been widely applied in military communications. The development of spread spectrum techniques was motivated by the need to combat intentional jamming and also to conceal transmission [2]. In commercial mobile communications, CDMA systems have many attractive properties such as interference suppression, a higher spectrum reuse factor, soft capacity, soft hand-over, wideband multipath diversity, and voice activity utilization [3]. For these reasons, CDMA has recently attracted much attention. One of the current second-generation cellular communications systems, IS-95, is based on narrowband DS-CDMA technology [3]. The most promising candidate for the new third-generation mobile communications systems, called International Mobile Telecommunications-2000 (IMT-2000), is wideband CDMA (W-CDMA) [4]-[7]. Recently the European Telecommunications Standards Institute (ETSI) decided to adopt W-CDMA technology for the frequency-division duplex (FDD) bands [8]. In Japan, the Association of Radio Industries and Business (ARIB), the standardization body of the radio sector, is now developing a W-CDMA air interface standard [9].

DS-CDMA is the most popular of CDMA techniques. The DS-CDMA transmitter multiplies each user's signal by a distinct code waveform. The detector receives a signal composed of the sum of all user's signals, which overlap in time and frequency. In conventional DS-CDMA systems, a particular user's signal is detected by correlating the entire received signal with that user's code waveform. The conventional DS-CDMA detector suffers from two major drawbacks: the near-far problem and an interference limitation on network capacity. The near-far problem is a situation in which users near the receiver are received at higher powers than those far away, and those further away suffer a degradation in performance, i.e. bit-error-rate (BER). The conventional detector consists of a matched filter and a decision device. Since the output of each matched filter contains a spurious component which is linear in the amplitude of each of the interfering users, the strongest user often severely interferes with the other users. Consequently, the BER and anti-jamming capability of the weakest user are degraded substantially. Thus, in order to maintain an acceptable level of bit-error-rate for all user, DS-CDMA often requires strict control over transmitter power for each user, which is often very difficult to realize. The interference limitation refers to the fact that the number of simultaneous users is limited to approximately 10% of the processing gain, even for the case of perfect power control [3]. These drawbacks, caused by the fact that single-user detection treats multiuser interference as noise, severely impair the performance of the CDMA system.

Because of the interference among users, however, a better detection strategy

would be to use multiuser detection (also referred to as joint detection or interference cancellation). Here, information about multiple users is used jointly to better detect each individual user. The work of Verdú [10]-[13] has shown that an optimum maximum likelihood multiuser detector can achieve optimum near-far resistance and a significant performance improvement over the conventional (single user) detector. The improvement, however, is obtained at the expense of a dramatic increase in computational complexity, which grows exponentially with the number of users. Thus, when the number of users is large, the optimum detector becomes infeasible. Thus, many suboptimum multiuser detectors have been proposed [12]-[19] to offer better performance complexity tradeoff.

The utilization of the multiuser detection algorithms has the potential to provide higher spectrum utilization efficiency and better performance for DS-CDMA systems. The number of users jointly decoded in the DS-CDMA systems could be very large, since each user occupies the entire bandwidth and is thus fully overlapped with all other users. Multiuser detection may then only be feasible at the base station. In general, it is easier to apply multiuser detection into a system with short spreading codes since cross-correlation does not change every symbol as with long spreading codes.

1.2 Motivation and Objective

The optimal multiuser detector for CDMA systems is prohibitively complex for practical implementations. Therefore, several linear suboptimum multiuser detectors have been proposed which can be characterized as an inverse of some form of correlation matrices. If the correlation changes, the detectors must be redesigned. An ideal computation of the decorrelating or the LMMSE detector requires an order of K^3 flops[1] for asynchronous CDMA systems [73] or K^2 flops for synchronous CDMA systems [74], where K is the number of users. To alleviate this computational complexity, many researchers have recently focused on adaptive, decentralized[2], multiuser detectors. One problem associated with these adaptive multiuser detectors is that the optimum weights are not achieved in practice, even if the step-size is optimal. Also the finite training period required in these adaptive detectors, together with high system loads (the ratio of users to processing gain close to one), set some constraints on the achieved MSE, especially in near-far environments. As a result, the adaptive multiuser detector usually experiences significant performance degradation compared with its optimum MMSE multiuser receiver at high system loads. Due to the above mentioned problems of the adaptive multiuser receivers based on linear filtering, nonlinear adaptive multiuser detection has gained a considerable attention for its potential capacity increase and simplicity. The main objective of this thesis is to develop a low complexity adaptive multistage detection scheme that can improve

[1] A floating point operation (flop) is defined to be a multiplication or an addition ([91, p. 19]).

[2] Centralized multiuser detectors make a joint detection of the symbols of different users. Decentralized multiuser detectors (sometimes also called single-user detectors) demodulate a signal of one desired user only.

both the convergence speed and the BER performance of the conventional adaptive multiuser receiver in both AWGN and fading channels.

It was shown in [81] that a class of MMSE decision feedback detectors (MMSE-DFDs) are relatively simple and can perform significantly better than linear MMSE multiuser detectors. Most of the work up to this point dealing with the MMSE-DFD and its adaptive implementations has assumed either an AWGN channel [83] or a slowly time-varying multipath fading channel [84]. Up to the authors' best knowledge, the MMSE-DFD for relatively fast fading channels has not been presented. Therefore, the second goal is to design a nonlinear adaptive MMSE-DFD which can operate in fast fading channels and perform better than its linear counterpart.

1.3 Thesis Contribution

This thesis presents three different nonlinear adaptive multiuser detection schemes that can significantly increase the spectral efficiency of the DS-CDMA systems over their linear counterparts. The main contributions of this thesis are listed as follows:

- For DS-CDMA systems in AWGN channels, we propose a blind adaptive MMOE-PIC multiuser detector which performs very close to the centralized optimum LMMSE detector and has a much simpler computational complexity.

- For the more interesting case of fading channels, we introduce a nonlinear multistage LCMV-HD-PIC detection scheme which yields a near-optimum BER performance using only a few stages. The performance of the proposed detector

is also shown to be insensitive to the system loads in flat fading channels.

- For the DS-CDMA systems in fast-fading channels, we present a nonlinear successive decision-feedback multiuser detector based on the modified MMSE criterion. The proposed nonlinear detector is suitable for adaptive implementation in fast-fading channels and can achieve a spectral efficiency which is significantly higher than that of its linear counterpart. The performance loss of the proposed nonlinear detection introduced by the modified MMSE optimization function is also negligible, in contrast with the modified LMMSE detection.

1.4 Thesis Outline

Chapter 2 includes a review of multiuser detection in additive white Gaussian noise (AWGN) channels. A synchronous DS-CDMA multiuser system description is given. Several different multiuser detection schemes are reviewed. On one hand, the conventional detector is vulnerable to the near-far problem. On the other hand the computational complexity of the optimum detector is so high that is infeasible, at least with existing technology. We then review two main classes of suboptimal detectors that have been proposed: linear multiuser detectors and subtractive interference cancellation multiuser detectors. Previous work on the multiuser detection in the literature is also presented. The significance of the multiuser detection and its advantage are pointed out.

In chapter 3, a modified multistage parallel interference cancellation structure

based on the blind adaptive MMOE algorithm is introduced for DS-CDMA systems in AWGN channels. The complexity of the proposed receiver structure is shown to be linear in the number of users and hence, a much lower complexity than the centralized LMMSE multiuser detector. The proposed receiver utilizes soft decision (SD) of the conventional blind adaptive MMOE detector on the interfering users' symbols when forming the MAI estimate. It is demonstrated that the proposed algorithm can significantly reduce the long training period required by the standard adaptive MMOE receiver in near-far environments. Furthermore, the BER of the proposed MMOE-PIC detector is analyzed and approximated using the Gaussian approximation. Both numerical and theoretical results show that the proposed receiver performs close to the optimum LMMSE receiver whereas the conventional adaptive MMOE detector suffers from high BER's due to the imperfect filter coefficients.

Chapter 4 introduces an adaptive multistage detection scheme with low complexity for DS-CDMA systems in the presence of time- and frequency- selective fading. The first stage is a blind adaptive multiuser detector based on the linear constrained minimum variance (LCMV) criterion. The interference cancellation occurs in the following stages. Our aim is to study the performance of the proposed algorithm and investigate techniques for efficient multistage detection for CDMA systems in fading channels. The simulation results show that the BER performance of the proposed algorithm approaches to the single user bound and is independent of system loads in flat fading channels. For multipath fading channels, from low to moderate SNR's, the performance of the proposed detector is within 1 dB (in SNR) of the single user bound

at moderate system loads. On the other hand, the BER of the proposed receiver is shown to exhibit an error floor at high SNR's due to the poor MAI estimates.

Chapter 5 focuses on a class of nonlinear MMSE decision-feedback multiuser receivers which are known to offer a large performance improvement relative to linear MMSE-based detection. A 2-stage modified MMSE decision-feedback multiuser detector is proposed for frequency-selective fast-fading channels. Considering a multipath fast-fading channel, the modified nonlinear adaptive receiver is shown to offer much higher gain than existing precombining linear MMSE receivers [77]. Considering a fixed multipath channel, and different system loads, we demonstrate that the difference in performance between the proposed precombining nonlinear receiver and its postcombining version is relatively small and fairly fixed over different system loads. Finally, we present convergence results for the proposed nonlinear adaptive receiver and compare it with the precombining LMMSE adaptive receiver [77].

In Chapter 6 a brief summary of the accomplished work, with an emphasis on the contributions to the area of multiuser detection is presented. Some possible extension of this work and directions of future research are also presented.

Chapter 2

Review of Multiuser Detection

Recently, there has been a great interest in improving DS-CDMA detection through the use of multiuser detection. In multiuser detection, code and timing (and possibly amplitude and phase) information of multiple users are jointly used to detect each user signal. The main assumption in these detection techniques is that the codes of the multiple users are known to the receiver a priori. In [10], Verdú proposed and analyzed the optimum multiuser detector, or the maximum likelihood sequence (MLS) detector (described later in this chapter). Even though the MLS detector offers a substantial gain over the conventional matched filter receiver, its computational complexity is too high for practical DS-CDMA systems. Therefore, over the last decade or so, most of the research has focused on finding suboptimum multiuser detectors which are more feasible to implement.

In general, the proposed suboptimum detectors can be classified in one of the two categories: linear multiuser detectors [13] and subtractive interference cancellation

detectors [14]. In linear multiuser detection, a linear mapping (transformation) is applied to the soft outputs of the conventional detector to provide a set of outputs, which hopefully provide better performance. In subtractive interference cancellation detection, estimates of the interference are generated and subtracted out. We will review several important detectors in each category in this chapter.

An outline of this chapter is as follows. In Section 2.1 the synchronous DS-CDMA multiuser system model is presented. In Section 2.2, we describe the idea behind multiuser detection. Section 2.3-2.8 investigate six multiuser detection schemes: the conventional, the optimum, the decorrelating, the LMMSE, the serial interference cancellation (SIC) detectors and the multistage parallel interference cancellation detectors, respectively. Finally, Section 2.9 concludes this chapter.

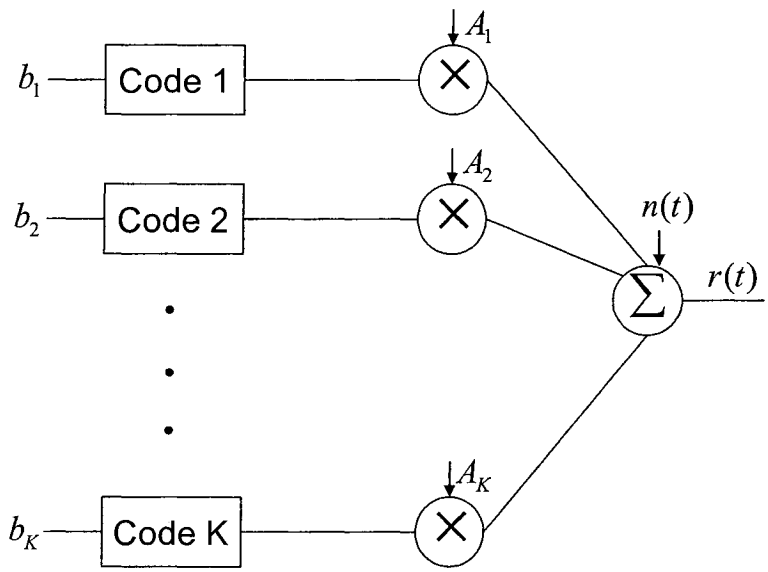

Figure 2.1: A synchronous DS-CDMA system model

2.1 Multiuser System Description

2.1.1 System Model

We consider a synchronous DS-CDMA system which is shown in Figure 2.1. All users share the same bandwidth. The signaling interval of each user is T seconds, and the input alphabet is antipodal binary: $\{+1, -1\}$. The transmitted baseband signal due to the kth user is given by

$$r_k(t) = \sum_{i=-\infty}^{\infty} A_k e^{j\theta_k} b_k(i)\, s_k(t - iT) \tag{2.1}$$

where $b_k(i)$ is the ith time-independent and equiprobable symbol transmitted by the kth user. A_k and θ_k are the signal amplitude and phase shift of user k, respectively. $s_k(t)$ is the kth user signature waveform which is assumed to have a unit energy ($\int_0^T \|s_k(t)\|^2\, dt = 1$). For DS-CDMA, this spreading waveform can be written as

$$s_k(t) = \sum_{i=0}^{N-1} p_k[i]\, \Psi(t - iT_c) \tag{2.2}$$

where $\Psi(t)$ is the chip pulse shape, T_c is the chip duration, $N = T/T_c$ is the processing gain and $p_k[i] \in \left\{\pm 1/\sqrt{N}\right\}$, $i = 0, ..., N-1$, is the real-valued spreading sequence. In the reminder of this dissertation we take $\Psi(t)$ to be a square pulse on the interval $[0, T_c)$, but there is no fundamental reason why a different chip pulse shape could not be used. Because short spreading codes are required for the adaptive algorithms considered in this thesis, It is assumed that the same spreading waveform is used for

each symbol.

At the receiver side the received baseband signal is the noisy sum of all users' signals. Considering a K-user system, the received multiuser signal is given by

$$r(t) = \sum_{k=1}^{K} \sum_{i=-\infty}^{\infty} A_k b_k(i)\, s_k(t - iT) + n(t) \tag{2.3}$$

where $n(t)$ is the complex addictive white Gaussian noise with two-sided power spectral density σ_n^2. According to (2.1), each user's signal travels along a single path, so the model does not illustrate multipath propagation. The effect of multipath is discussed in Chapter 4.

The received signal in (2.3) is sampled at the output of the chip matched filter at a rate of $T_c^{-1} = N/T$. If we let $\mathbf{r}(i)$ be the N-vector containing samples during the ith transmitted symbol, we can write

$$\mathbf{r}(i) = \mathbf{SAb}(i) + \mathbf{n} \tag{2.4}$$

where $\mathbf{S} = [\mathbf{s}_1, \mathbf{s}_2, ..., \mathbf{s}_K]$ and $\mathbf{s}_k$ is the column vector of spreading sequence associated with user k, $\mathbf{A} = diag[A_1 e^{j\theta_1}, A_2 e^{j\theta_2}, ..., A_K e^{j\theta_K}]$, $\mathbf{b}(i) = [b_1(i), b_2(i), ..., b_K(i)]^T$ is the data vector where "T" denotes matrix transpose, and $\mathbf{n}$ is the complex channel noise vector with covariance $\sigma_n^2\mathbf{I}$ where $\mathbf{I}$ is $K \times K$ diagonal matrix.

For the rest of this chapter, we will consider a very simplified DS-CDMA system. A number of simplifications will be exposed in the rest of the dissertation. These assumptions are as follows:

- We consider a channel with real attenuation. The real model is convenient for analyzing coherent methods, and can be easily generalized to the complex case. Under this real attenuation assumption, the received amplitude matrix $\mathbf{A} = diag[A_1, A_2, ..., A_K]$. In Chapter 4 and 5, we extend our treatment to multiuser detection for fading channels, where complex attenuation need to be considered.

- Certain parameters are assumed to be known perfectly. The multiuser detectors presented in this chapter and Chapters 4 and Chapter 5 take advantage of the known channel parameters so that amplitudes, phase and delays do not appear in treatment at all.

2.1.2 Spreading Codes

In Chapter 3 and Chapter 4, we have chosen a set of Gold sequences each of length 31 chips as the spreading codes assigned to different users. In chapter 5, a family of Gold sequences with processing gain 15 is employed in order to simplify the simulations although the choice of length 15 does not offer good periodic cross-correlations.

Appendix A shows the Gold codes as well as their auto-correlation and cross-correlation properties. As shown in the Appendix, the length N, of a Gold sequence is equal to $2^m - 1$, where m is an integer. The total number of Gold sequences with length N is always $N + 2$ [25].

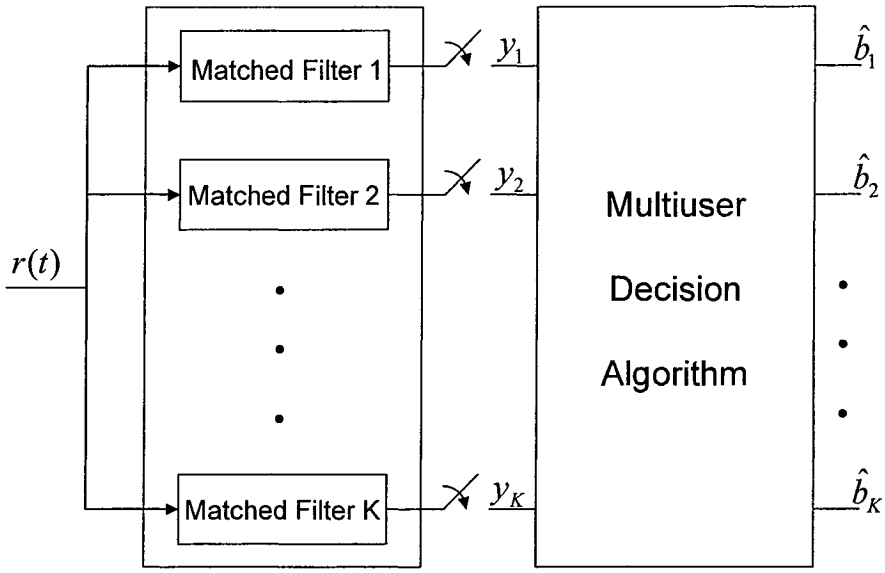

Figure 2.2: CDMA multiuser detection concept

2.2 Multiuser Detection Concepts

The first CDMA interference cancellation references can be found in [20]-[24]. In these works, a number of ideas that are present are still in much of the ongoing research. Estimates based on mean-squared-error and maximum likelihood are discussed in [20]. Later on, the detection scheme proposed in that paper was known as the decorrelating detector. In [20], however, it was erroneously shown that this detector is optimum in terms of bit-error-rate. Reference [24] shows how cancellation is implemented by solving simultaneous equations, in essence, by inverting a key matrix. Significant theoretical steps were taken in [10] and [11] by Verdú, in analyzing the structure and complexity of optimal multiuser receivers. This work also initiated a new research on suboptimal multiuser detection.

Multiuser detectors commonly have a front-end whose objective is to obtain a discrete-time process from the received continuous-time waveform $r(t)$. Continuous-to-discrete-time conversion can be realized by conventional sampling, or more generally, by correlation of $r(t)$ with deterministic signals. Therefore, the first step in the multiuser detection process is to pass the received signal $r(t)$ through a bank of matched filters (or correlators). The bank of matched filters consists of K filters matched to individual spreading codes of the same system followed by samplers as shown in Figure 2.2.

For synchronous CDMA, the output of the kth matched filter (which is matched to the spreading code of kth user) at the sampling time is given by

$$\begin{aligned} y_k &= \int_0^T r(t)s_k(t)dt \\ &= \int_0^T s_k(t)\left[\sum_{v=1}^{K} A_v b_v s_v(t) + n(t)\right] dt \\ &= A_k b_k + \sum_{v=1, v\neq k}^{K} A_v b_v R_{k,v} + \int_0^T s_k(t)n(t)dt \end{aligned} \tag{2.5}$$

where

$$R_{k,v} = \int_0^T s_k(t)s_v(t)dt \tag{2.6}$$

is the cross-correlation between the spreading codes assigned to user k and user v. Note that y_k consists of three terms. The first term is the desired user's information. The second term is the result of the multiple access interference, and the last term

is due to the noise. Schneider [20] showed that the outputs of the bank of matched filters form a set of sufficient statistics for demodulating the input sequence $b(i)$ from the received signal $r(t)$, i.e., that no additional relevant information can be extracted from the remaining noise process $n^{\emptyset}(t) = n(t) - \sum_{k=1}^{K} \int_0^T s_k(t)n(t)dt$ and $n^{\emptyset}(t)$ is uncorrelated with the outputs of the bank of matched filters $\{y_k\}$.

It is convenient to express (2.5) in a vector form given by

$$\mathbf{y} = \mathbf{RAb} + \mathbf{z} \tag{2.7}$$

where $\mathbf{R}$ is the normalized cross-correlation matrix with elements $R_{k,v}$, $\mathbf{y} = [y_1, y_2, ..., y_K]^T$, and $\mathbf{n}$ is a zero-mean Gaussian random vector with covariance matrix equal to

$$E[\mathbf{n}\mathbf{n}^T] = \sigma_n^2\mathbf{R} \tag{2.8}$$

2.3 Conventional Detector

In the following sections we briefly review several previously proposed multiuser detectors of interest. Before doing so, we begin our discussion with the simplest detector, namely, the conventional detector.

The conventional detector for the received signal is described in (2.5), which is a

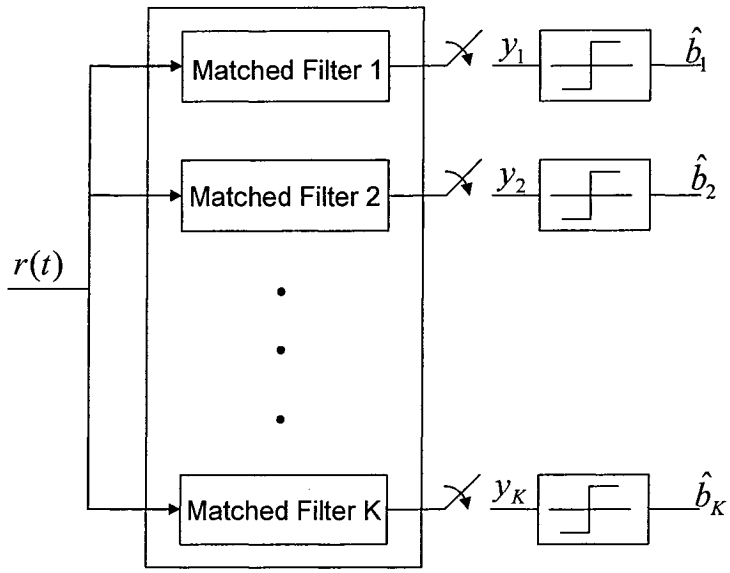

Figure 2.3: Conventional (single-user) detector

bank of K correlators, as shown in Figure 2.3. Here, each code waveform is regenerated and correlated with the received signal in a separate detector branch. The correlation detector can be equivalently implemented through what is known as matched filter [25]. Thus, the conventional detector is often referred to as the matched filter receiver. The outputs of the correlators (or matched filters) are sampled at bit times, which yields "soft" estimates of the transmitted data. The final ± 1 "hard" data decisions are made according to the signs of the soft estimates as shown below

$$\hat{b}_k = sgn(y_k) \tag{2.9}$$

Note that the conventional detector ignores MAI and treats it as noise. Thus, the existence of MAI has significant impact on the capacity and performance of the

conventional direct-sequence system. In [26], the kth user probability of error for the conventional detector was obtained as

$$P_k^c = \frac{1}{2^{K-1}} \sum_{\mathbf{b}\in\{-1,+1\}^K, b_k=1} Q\left(\frac{A_k - \sum_{v=1,v\neq k}^{K} A_v b_v R_{k,v}}{\sigma_n}\right) \tag{2.10}$$

where $Q(x)$, $\frac{1}{\sqrt{2\pi}} \int_0^\infty e^{-t^2/2} dt$. When the MAI terms (2.10) are significant, the BER of this detector can be very high. This is due to the fact that MAI depends both on the cross-correlation between sequences and the energies, $A_1, A_2, ...A_K$.

It is clear from Figure 2.3 that the conventional detector follows a single-user detector strategy; each branch detects one user without regard to the existence of the other users. Thus, there is no sharing of multiuser information or joint signal processing (i.e., multiuser detection).

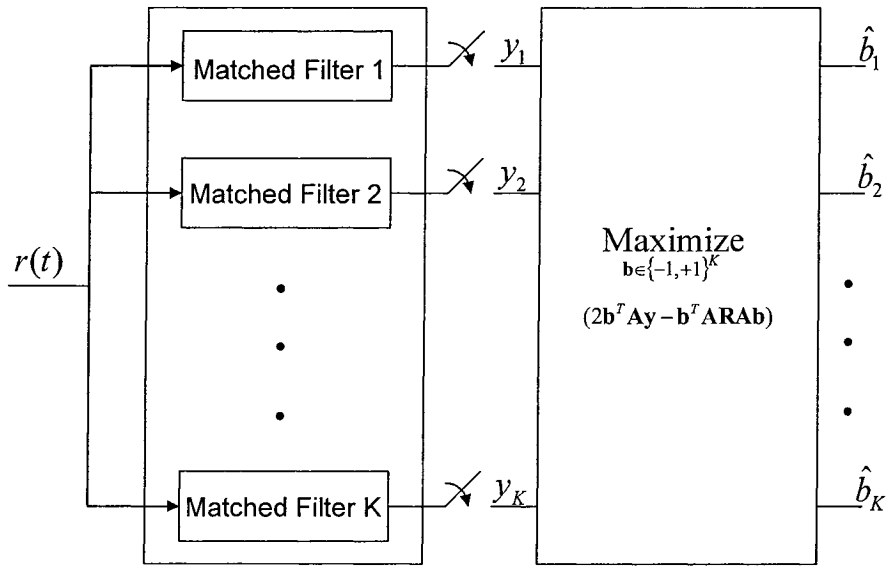

Figure 2.4: Optimum multiuser detector

2.4 Optimum Detector

The optimum multiuser detector, which is proposed by Verdú in [27], is defined as a detector that selects the set of symbols corresponding to that signal among the possible ones which resembles most closely, in the maximum likelihood sense, the received signal. Furthermore, if all vectors $\mathbf{b}$ are a priori equiprobable, then the minimum distance rule gives the maximum-a-posteriori (MAP) decision. The optimum multiuser detector, thus can be expressed mathematically as [27]

$$\hat{\mathbf{b}} = \arg \max_{\mathbf{b}\in\{-1,+1\}^K} \left\| r(t) - \sum_{v=1}^{K} A_v b_v s_v(t) \right\|. \tag{2.11}$$

For synchronous CDMA systems, (2.11) may be written as

$$\begin{aligned} \hat{\mathbf{b}} &= \arg \max_{\mathbf{b}\in\{-1,+1\}^K} \int_0^T \left[r(t) - \sum_{v=1}^{K} A_v b_v s_v(t) \right]^2 dt \\ &= \arg \min_{\mathbf{b}\in\{-1,+1\}^K} \int_0^T r^2(t)dt - 2\sum_{v=1}^{K} A_v b_v \int_0^T r(t)s_v(t)dt \\ &\quad + \sum_{u=1}^{K}\sum_{v=1}^{K} A_u b_u A_v b_v \int_0^T s_u(t)s_v(t)dt \end{aligned} \tag{2.12}$$

or equivalently in matrix notation as

$$\hat{\mathbf{b}} = \arg \max_{\mathbf{b}\in\{-1,+1\}^K} \left(2\mathbf{b}^T\mathbf{A}\mathbf{y} - \mathbf{b}^T\mathbf{A}\mathbf{R}\mathbf{A}\mathbf{b}\right) \tag{2.13}$$

Equation (2.13) dictates an exhaustive search over 2^K possible combinations of the components of the bit vector $\mathbf{b}$. Despite the huge capacity and performance gains

offered by the MLS detector over the conventional receiver, the optimum multiuser detector is impractical since its computational complexity grows exponentially in the number of users. A realistic direct-sequence system has a relatively large number of active users. Thus, the exponential complexity in the number of users makes the cost of this detector too high. In the following sections, we look at various suboptimum multiuser detectors that are simpler to implement.

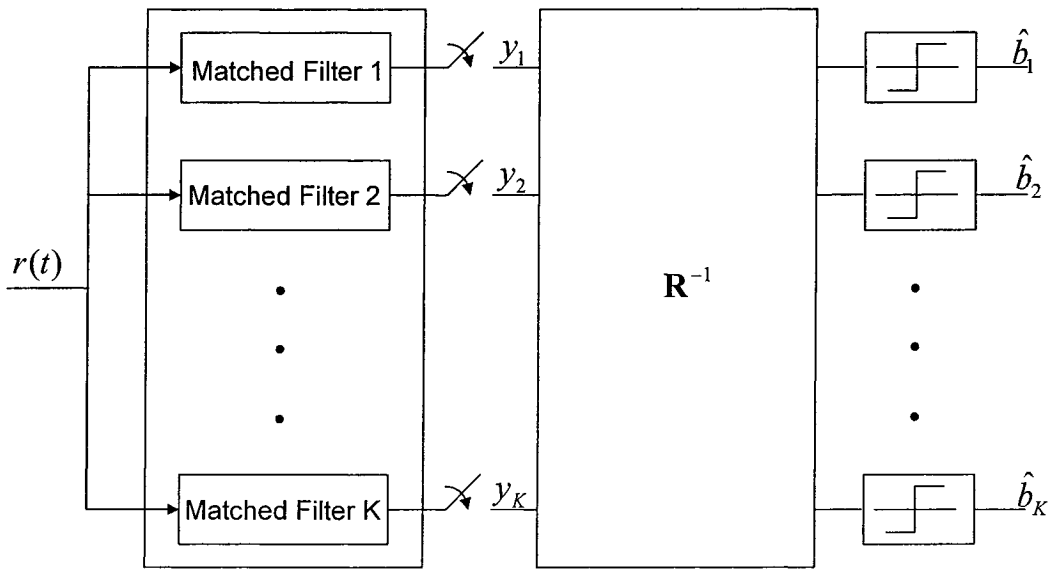

Figure 2.5: Decorrelating multiuser detector

2.5 Decorrelating Detector

The decorrelating detector shown in Figure 2.5 applies the inverse of the correlation matrix $\mathbf{R}^{-1}$ to the conventional detector output in order to decouple the data. Thus,

the soft estimate of this detector is

$$\hat{\mathbf{y}} = \mathbf{R}^{-1}\mathbf{y} = \mathbf{A}\mathbf{b} + \mathbf{R}^{-1}\mathbf{z} \tag{2.14}$$

and the decision is

$$\hat{\mathbf{b}} = sgn(\hat{\mathbf{y}}). \tag{2.15}$$

Thus, we see that the decorrelating detector completely eliminates the MAI. This detector is very similar to the zero-forcing equalizer [25] which is used to completely eliminate intersymbol interference (ISI).

The decorrelating detector was initially proposed in [20, 24]. It was extensively analyzed by Lupas and Verdú in [12, 13] for coherent detection. In addition, the idea of decorrelation has also received considerable attention in [28]-[32] where the noncoherent version of the decorrelator was obtained. The decorrlating detector has several desirable features. Foremost among these properties are:

- It offers significant performance/capacity gains over the conventional detector.
- It does not require the knowledge of the users' energies, and thus its performance is independent of the energies of the interfering users. This can be seen form (2.14). The only requirement is the knowledge of timing which is anyway necessary for the code despreading at the centralized receiver.
- It has computational complexity significantly lower than that of the optimum

multiuser detector. The per-bit complexity is linear in the number of users, excluding the costs of recomputation of the inverse mapping.

A disadvantage of this detector is that it causes noise enhancement. The power associated with the noise term $\mathbf{R}^{-1}\mathbf{z}$ at the output of the decorrelating detector is always greater than or equal to the power associated with the noise term at the output of the conventional detector for each bit [28]. As it is shown in [26], the error rate of the decorrelator is given by

$$P_k = Q\left(\frac{A_k}{\sigma_n\sqrt{(\mathbf{R}^{-1})_{k,k}}}\right). \tag{2.16}$$

Thus, we see that the performance of the decorrlating detector degrades as the cross-correlations between users increase. A more significant disadvantage of the decorrelating detector is that the computations needed to invert the matrix $\mathbf{R}$ are difficult to perform in real time. For synchronous systems, the problem is somewhat simplified: we can decorrelate one bit at a time. In other words, we can apply the inverse of a $K \times K$ correlation matrix. For asynchronous systems, however, the size of $\mathbf{R}$ is $NK \times NK$, which is quite large for a typical message length N.

2.6 MMSE Detector

Based on the more classical minimum mean-squared-error criterion, LMMSE multiuser detectors were derived and their performance was studied for both synchronous and asynchronous channels in [19] and [33]-[35]. This detector implements linear

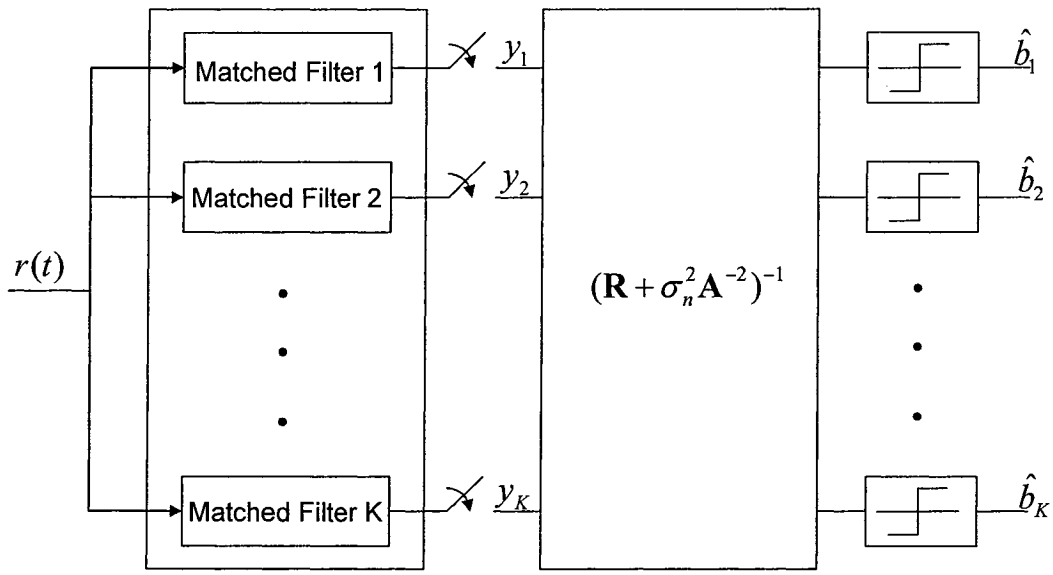

Figure 2.6: MMSE multisuser detector

mapping which minimizes the mean-squared-error between the actual data and the soft output of the MMSE detector. This linear MMSE detector (Figure 2.6) is given by [19]

$$\mathbf{W}_{MMSE} = \left[\mathbf{R} + \sigma_n^2 \mathbf{A}^{-2}\right]^{-1}. \tag{2.17}$$

Thus, the soft estimate of the MMSE detector is simply

$$\hat{\mathbf{y}} = \mathbf{W}_{MMSE}\mathbf{y}. \tag{2.18}$$

As can be seen, the MMSE detector implements a partial or modified inverse of the correlation matrix. The amount of modification is directly proportional to the background noise. The higher the noise level is, the less complete an inversion of $\mathbf{R}$ can be done without noise enhancement causing performance degradation. Because it takes the background noise into account, the MMSE detector generally provides better BER performance than decorrelating detector. As the background noise goes to zero, the MMSE detector converges in performance to the decorrelating detector. An important feature of MMSE detection is that it lends itself to adaptive implementations more readily than the decorrelating detector. The adaptive multiuser detector based on the MMSE criterion as in [36]-[38] eliminates the need to know the signature waveforms, time and amplitudes but needs to have training data sequences for every active user for initial adaptation.

An important disadvantage of the MMSE detector is that, unlike the decorrelating detector, it requires estimation of the received amplitudes. Another disadvantage is that its performance depends on the powers of the interfering users [19]. Therefore, there is some loss of resistance to the near-far problem as compared to the decorrelating detector. Moreover, while decorrelating and MMSE strategies are at once simple and attractive from a performance standpoint for low–moderate cross-correlations, their performance can degrade substantially for systems with higher bandwidth efficiencies. The problem here is that the structural constraint that the detector be linear, is too severe [89].

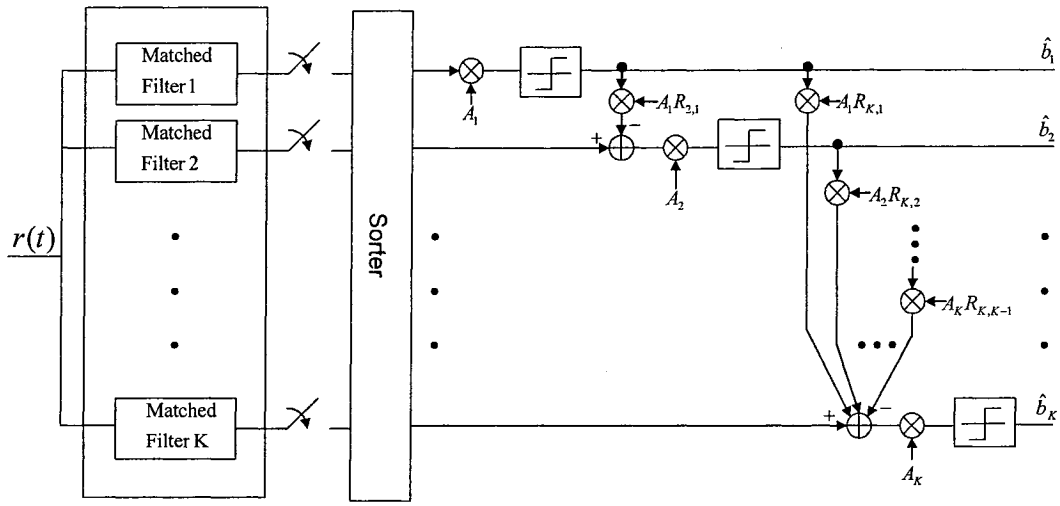

Figure 2.7: Successive interference cancellation detector

2.7 Successive Interference Cancellation

Here we review a class of subtractive interference cancellation detectors. The basic principle underlying these detectors is the creation used at the receiver to estimate the MAI contributed by each user. The bit decisions used to estimate the MAI can be hard or soft. The soft decision approach uses soft data estimates for the joint estimation of the data and amplitude, and is easier to implement. The hard decision approach feeds back a bit decision and is nonlinear. It requires reliable estimates of the received amplitudes in order to regenerate estimates of MAI. On the other hand, if reliable amplitude estimation is available, hard-decision subtractive interference cancellation generally outperforms soft-decision techniques. We briefly review several subtractive interference cancellation detectors below.

The successive interference cancellation detector [39, 40] involves detection of

users's signals in a given order. The first user is detected by regarding the interference from other users as noise. The detected and regenerated symbols of the first user are then subtracted from the received data and the second user is detected by regarding the interference from the remaining users as noise, and so on.

A diagram of the SIC detector is shown in Figure 2.7, where a hard decision approach is assumed. In each time frame, decisions are made in the order of decreasing user's strength, i.e., the stronger user makes decisions first, allowing the weaker users to utilize these decisions. The sorting is performed before the interference cancellation occurs. Thus, the decision for the kth user is given by

$$\hat{b}_k = sgn(y_k - \sum_{v=1}^{k-1} b_v R_{v,k} A_v). \tag{2.19}$$

The reasons for cancelling the signals in a descending order of their strengths are straightforward. First, it is easy to achieve acquisition and demodulation on the strongest users (best chance of a correct data decision). Second, the removal of the strongest users gives the most benefit for the remaining users. The result of this algorithm is that the stronger user will not benefit from any MAI reduction. The weakest users, however, will potentially see a huge reduction in their MAI.

A shortcoming of the successive cancellation is that its performance is asymmetric: equal-power users are demodulated with disparate reliability since the order in which users are cancelled greatly affects the performance of successive cancellation for a particular user. In next section, we explore a symmetrized version of successive

cancellation, which mitigates some of the shortcomings of that technique.

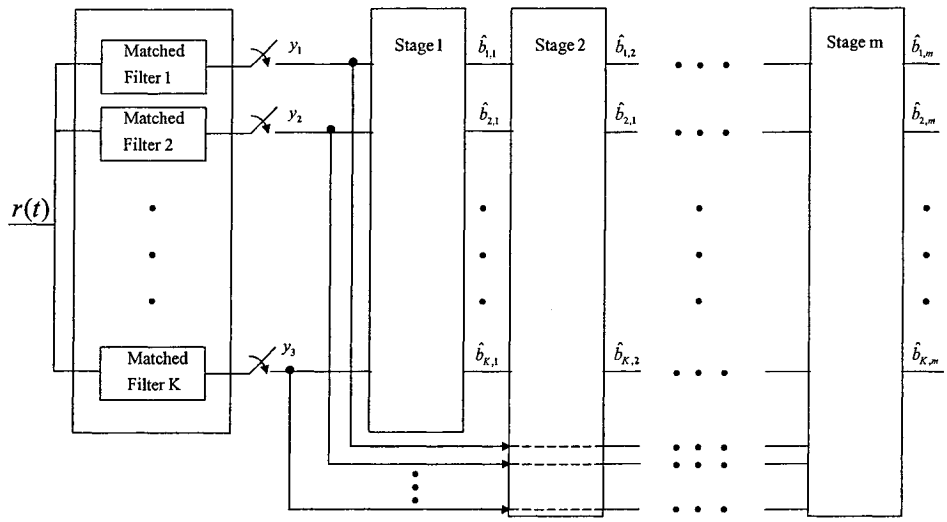

Figure 2.8: Multistage multiuser detector

2.8 Multistage Parallel Interference Cancellation

A multistage parallel interference cancellation detector is shown in Figure 2.8. This detector, proposed in [14, 15], uses (2.20) instead of (2.13)

$$\hat{b}_{m+1,k} = \arg \max_{b_k \in \{-1,+1\}, b_v = \hat{b}_{m,v}, v \neq k} \left(2\mathbf{b}^T\mathbf{A}\mathbf{y} - \mathbf{b}^T\mathbf{A}\mathbf{R}\mathbf{A}\mathbf{b}\right). \tag{2.20}$$

For $m > 1$, it is easy to show that

$$\hat{b}_{m+1,k} = sgn(\hat{y}_{m,k}) \tag{2.21}$$

where $\hat{y}_{m,k}$ is the mth stage statistic for the kth user and is given by

$$\hat{y}_{m+1,k} = y_k - \sum_{v=1, v\neq k}^{K} \hat{b}_{m,v} A_v R_{v,k}. \tag{2.22}$$

In demodulating the information bits of all users, the maximization of (2.20) is performed for each $k = 1, 2, ...K$. The $(m+1)$th stage estimate of $\mathbf{b}$ can be written as the sign of the mth stage vector of $\hat{\mathbf{y}}_m = [\hat{y}_{m,1}, \hat{y}_{m,2} \cdots \hat{y}_{m,K}]^T$ so that

$$\hat{\mathbf{b}}_{m+1} = sgn(\hat{\mathbf{y}}_m) = sgn[\mathbf{y} - (\mathbf{R} - \mathbf{I}_K)\mathbf{A}\hat{\mathbf{b}}_m]. \tag{2.23}$$

From (2.7), one can see that

$$\mathbf{y} = \mathbf{RAb} + \mathbf{z} = \mathbf{Ab} + \mathbf{M_I(b)} + \mathbf{z} \tag{2.24}$$

where $\mathbf{M_I(b)}$, $(\mathbf{R} - \mathbf{I}_K)\mathbf{Ab}$ represents the MAI vector. Substituting (2.24) in (2.23), the expression for the $(m+1)$th stage estimate of $\mathbf{b}$ is given by

$$\hat{\mathbf{b}}_{m+1} = sgn(\hat{\mathbf{y}}_m) = sgn[\mathbf{Ab} + \mathbf{M_I(b)} - \mathbf{M_I}(\hat{\mathbf{b}}_m) + \mathbf{z}]. \tag{2.25}$$

The result in (2.25) has a simple interpretation. The $(m+1)$th stage estimate of $\mathbf{b}$ is obtained as the sign of the mth stage statistic which in turn is obtained by subtracting from the sufficient statistic $\mathbf{y}$, the estimate of the MAI based on the mth stage estimate of $\mathbf{b}$.

A potential problem with the subtractive interference cancellation detector occurs when the initial data estimates are not reliable. In this case, even if the timing, amplitude, and phase estimates are perfect, if the bit estimate is wrong, the interfering effect of that bit on the signal-to-noise ratio is quadrupled in power (the amplitude doubles, so the power quadrupled). This is also known as hang-up phenomenon where the decision errors propagate to MAI estimates resulting in a detrimental effect on other users' decisions.

A number of studies have investigated PIC detection, such as [41]-[43]. In particular, [43] proposed a partial PIC scheme which takes into account the fact that the tentative decisions of the earlier stages are less reliable than those of the laster stages. Huge gains in performance and capacity are reported over the standard PIC detector. This recently proposed detector may be the most powerful of the subtractive interference cancellation detectors, and needs to be studied further.

2.9 Conclusion

In this chapter, a synchronous DS-CDMA system model was given. Then, we studied the idea behind multiuser detection. Finally, six previously proposed detection schemes were reviewed. It was shown that multiple access interference significantly limits the performance and capacity of the conventional DS-CDMA systems. The optimum MLS multiuser detector can provide huge gains in performance and capacity over conventional detector but is too complex to implement for practical DS-CDMA

systems. Among simpler suboptimum multiuser detectors, decorrelating and MMSE detectors provide optimum near-far resistance. Particularly, the decorrelating detector can be implemented without knowledge of the received amplitudes whereas the MMSE detector requires estimation of the received powers, but provides a better BER performance than decorrelating detector. Both the decorrelating and MMSE detectors require nontrivial computations that are a function of the cross-correlations. This is particularly difficult for the dynamic CDMA systems where the cross-correlations change each bit. On the other hand, a class of subtractive interference cancellation detectors has gained a considerable attention for its simplicity and potential capacity increase over conventional detector. These detectors attempt to estimate and subtract off the MAI in either serial or parallel approach. The subtractive interference cancellation detectors suffer from decision error propagation which may significantly reduce or even reverse the gains to be had from using these detectors.

Chapter 3

Blind Adaptive MMOE-PIC Detection

From the discussion in the previous chapter, it is clear that DS-CDMA with the conventional detector suffers from the near-far problem. The drawbacks of the conventional detector initiated efforts to develop more sophisticated receivers in which MAI is treated as part of information rather than noise. The study of the optimum detector showed that while superior performance over the conventional detector is possible, it can be obtained at a significant increase in computational complexity. Among the suboptimum multiuser detectors which were proposed to alleviate the complexity, the LMMSE receiver is receiving significant attention as it offers an attractive tradeoff between performance, complexity and the need for side information. However, the computation complexity of the optimum LMMSE receiver has cubic dependence on the number of users and is still too high for several applications. On the

other hand, the adaptive LMMSE receiver, which is simpler, suffers from significant performance degradation due to imperfect adaptation. In this chapter we introduce a new adaptive multistage PIC detection scheme. The new detector yields a near-optimum LMMSE performance, while its computational load is linear in the number of users.

The rest of the chapter is organized as follows. In Section 3.1 previous work in the area is summarized and the contribution of this chapter is reviewed. Section 3.2 thoroughly discusses the idea behind the proposed new detector, and gives performance analysis and simulation results in synchronous AWGN channels. The proposed algorithm and its performance in asynchronous channels are given in Section 3.3. Finally Section 3.4 presents a discussion and summarizes the results.

3.1 Introduction

3.1.1 Previous Work

To alleviate the computational complexity involved in centralized LMMSE multiuser detectors, many researchers have recently focused on blind adaptive, decentralized detectors (e.g., [45-47] and references therein). These blind methods have been introduced to eliminate the need for long training sequences. Among these blind techniques, Honig et al. [25] have proposed an adaptive MMSE receiver which can be realized in a blind mode based on the minimum mean-output-energy criterion.

One of the prominent suboptimal multiuser detectors that has attracted the attention of many researchers is the parallel interference cancellation scheme introduced in [14]. The reason behind this is due to its potential capacity increase and simplicity compared with other suboptimal detectors. Previous work on combining MMSE detection and PIC was presented earlier in [48], but no adaptive implementation was provided. Other related, but different, multistage feedback cancellers have been presented in [15] where the first stage is a decorrelator.

3.1.2 Contribution

Based on the work discussed in the previous section, we propose a blind adaptive MMOE-PIC algorithm for the uplink of a DS-CDMA system. As will be shown in the sequel, the proposed algorithm has a computational complexity that is shown to be linear in the number of users as opposed to the MMSE multiuser detector whose complexity has a cubic dependence on the number of users. In addition to this complexity feature, the blind adaptive MMOE-PIC, which utilizes soft decision to estimate MAI, requires no side information on the received signal amplitudes as the MMSE multiuser detector does. This added merit can further lower the complexity of the overall system. Further to the complexity issue, our combined MMOE-PIC algorithm is shown to improve both the convergence speed and the BER performance of the conventional blind adaptive MMOE detector in both synchronous and asynchronous systems. As will be shown later, the MMOE-PIC algorithm is able to successfully suppress strong interference components arising from near-far situations

and hence, performing close to the optimum LMMSE receiver.

3.2 Blind Adaptive MMOE-PIC Detector in Synchronous Channels

In this section, we propose a new adaptive multistage parallel interference cancellation scheme based on the blind adaptive MMOE algorithm in synchronous AWGN channels. The proposed algorithm exploits both the simplicity of the blind adaptive MMOE detector and the novel approach of a multistage detector in maximizing (2.13). In addition, the system model that we study in this section is the same as what we studied in Chapter 2.

In section 3.2.1, we briefly review the conventional blind adaptive MMOE receiver. Section 3.2.2 presents the proposed blind adaptive MMOE-PIC algorithm. Section 3.2.3 demonstrates the BER approximation for the proposed detector. Performance comparisons between the proposed detector and its conventional MMOE counterpart in near-far situations are discussed in section 3.2.4.

3.2.1 Blind Adaptive MMOE Detection

Here, we consider the linear detector with coefficients $\mathbf{w}$ that minimizes the output variance or MOE which is defined by

$$MOE = E\left[(\mathbf{w}^T\mathbf{r})^2\right] \tag{3.1}$$

It is clear from (3.1) that some constraint needs to be imposed when minimizing MOE in order to avoid the trivial solution $\mathbf{w} = \mathbf{0}$. In particular, it is desirable to constrain the response of the user of interest to a constant, in which case, minimization of the MOE results in minimization of the energy of the interference. The case where no multipath is present was studied in [44]. In that case, the constraint which guarantees no signal cancellation is given by

$$\mathbf{w}^T\mathbf{s} = 1 \tag{3.2}$$

where $\mathbf{s}$ is the column vector of spreading sequence. Now, consider a linear detector for user k, the achieved MSE is given by

$$\begin{aligned} MSE &= E\left[\left(A_k b_k - \mathbf{w}_k^T\mathbf{r}\right)^2\right] \\ &= E\left[(\mathbf{w}_k^T\mathbf{r})^2\right] - 2A_k E\left[\mathbf{w}_k^T\mathbf{r}b_k\right] + A_k^2 \\ &= MOE - A_k^2. \end{aligned} \tag{3.3}$$

Equation (3.3) shows that minimizing the MOE subject to the constraint (3.2) is equivalent to minimizing the MSE. The MMOE solution of the optimization problem in (3.1) and (3.2) is given by [44] as

$$\mathbf{w}_k = \frac{1}{\mathbf{s}_k^T\Gamma^{-1}\mathbf{s}_k}\Gamma^{-1}\mathbf{s}_k \tag{3.4}$$

where $\Gamma = E[\mathbf{r}\mathbf{r}^T] = \mathbf{S}\mathbf{A}^2\mathbf{S}^T + \sigma_n^2\mathbf{I}$.

The MMOE criterion has been applied in many signal processing areas, one of which is spatial filtering or beamforming [72]. The generalized sidelobe canceller (GSC) structure for adaptive beamforming represents an effective implementation of our blind MMOE multiuser detection by changing a constrained minimization problem into an unconstrained form. The basic idea is to decompose the weight vector $\mathbf{w}$ into two orthogonal part

$$\mathbf{w} = \mathbf{s} + \mathbf{x} \quad where \quad \mathbf{s}^T\mathbf{x} = 0. \tag{3.5}$$

Thus, the canonical representation in (3.5) suggests that the blind adaptive detector can be conveniently implemented as shown in Figure 3.1.

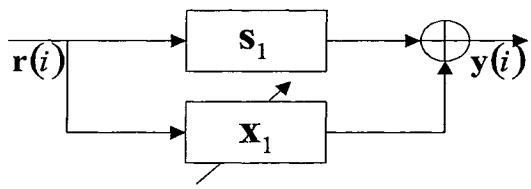

Figure 3.1: Blind adaptive detector with $\mathbf{x}_k$ governed by (3.8).

In order to derive the adaptive part, $\mathbf{x}$, of the blind MMOE detector, we need to compute the gradient of the MOE function in (3.1) which is given by

$$\nabla_{\mathbf{x}}(MOE) = 2P_{\mathbf{s}_k}^{\perp}\Gamma\mathbf{w}_k = 2(\mathbf{I} - \mathbf{s}_k\mathbf{s}_k^T)\Gamma\mathbf{w}_k \tag{3.6}$$

where $P_{\mathbf{s}_k}^{\perp} = (\mathbf{I} - \mathbf{s}_k\mathbf{s}_k^T)$ represents the subspace orthogonal to $\mathbf{s}_k$. From (3.6), a blind

stochastic adaptation mechanism can be derived by approximating the gradient with

$$\nabla_{\mathbf{x}}(MOE) = 2P^{\perp}_{\mathbf{s}_k}\Gamma\mathbf{w}_k \approx 2P^{\perp}_{\mathbf{s}_k}\mathbf{r}(i)\mathbf{r}^T(i)\mathbf{w}_k \approx 2P^{\perp}_{\mathbf{s}_k}\mathbf{r}(i)y_k(i). \tag{3.7}$$

Therefore, the stochastic gradient adaptation rule is

$$\mathbf{x}_k(i+1) = \mathbf{x}_k(i) - \mu(\mathbf{I} - \mathbf{s}_k\mathbf{s}_k^T)\mathbf{r}(i)y_k(i) \tag{3.8}$$

where μ is the step-size parameter and $y_k(i) = \mathbf{w}_k^T(i)\,\mathbf{r}(i)$ is the output of the adaptive detector.

It was shown in [44] that the blind gradient algorithm (3.8) suffers from noisy estimates when compared with the least mean square (LMS) algorithm [49] in the decision directed mode. Therefore, the optimum filter coefficients in (3.4) can not be achieved in practice. This results in a significant performance degradation, especially in systems with high loads and near-far problems.

3.2.2 Adaptive MMOE-PIC Algorithm in Synchronous Channels

We observe from (3.3) that the filter output, $y_k(i)$, represents an estimate of $A_k b_k(i)$. This estimate is obtained without the knowledge of either the data symbol or the user's signal amplitude. Thus this blind estimate together with the users spreading codes (assumed perfectly known), can allow us to perform linear cancellation on the

MAI. Note that the operation of the PIC algorithm alone requires signal amplitude estimation (for all users) plus early estimates for users' data to regenerate the MAI estimates. On the other hand, our proposed MMOE-PIC algorithm incorporates the MMOE to obtain these estimates and hence less computational complexity and improved system's performance as will be shown shortly. The improved performance is simply due to the combined MMOE-PIC multiuser interference rejection capability which is shown to effectively suppress MAI as compared to the blind adaptive MMOE algorithm.

Motivated by the above thought, we propose a new linear PIC structure where the blind adaptive MMOE algorithm is employed as the base decision function. Compared with the conventional PIC, the proposed algorithm is shown to effectively alleviate the effect of the hang-up phenomenon explained earlier. This of course results in a more stable performance and faster convergence rate.

The interference suppression of the MMOE-PIC algorithm is performed using a multistage linear PIC with soft symbol decisions obtained from the adaptive MMOE detector. The receiver structure is depicted in Figure 3.2. The output vector for the kth user at the ith symbol interval and the $(m+1)$th cancellation stage can be expressed as

$$\mathbf{r}_{[PIC]m+1,k}(i) = \mathbf{r}(i) - \mathbf{S}\Omega_{m,k}(i)\,\mathbf{y}_m(i) \tag{3.9}$$

where $\mathbf{y}_m(i) = [y_{m,1}(i), y_{m,2}(i), ..., y_{m,K}(i)]^T$, and $\Omega_{m,k}(i) \in [0,1]^{K\times K}$ is a diagonal

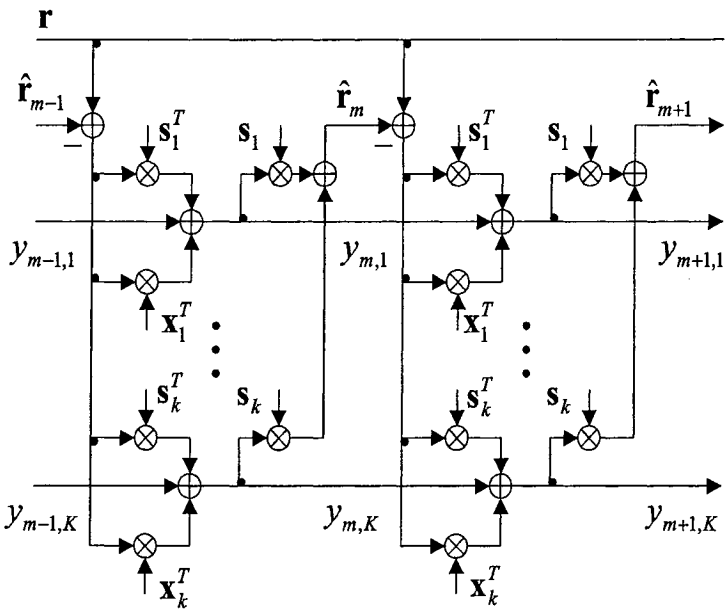

Figure 3.2: The MMOE-SD-PIC structure, stages m and (m+1) are shown.

matrix including weights for partial interference cancellation. The weight for the desired user is set to zero (i.e., $\gamma_{m,k}(i) = 0$). On the other hand, the weights $\gamma_{m,j}(i) \in [0, 1]$ for user $j \neq k$ depend on the estimated quality of the decision statistic for the corresponding user. In this work, however, a constant weight $\gamma_{m,j}(i) = 1$ is used for user $j \neq k$ at each stage throughout the cancellation process. Using the PIC algorithm, the discrete output signal $y_{m+1,k}(i)$ at the $(m + 1)$th IC iteration is given

by

$$
\begin{aligned}
y_{m+1,k}(i) &= \mathbf{w}_k^T(i)\mathbf{r}_{[PIC]m+1,k}(i) \\
&= \mathbf{w}_k^T(i)\left[\mathbf{r}(i) - \sum_{\substack{j=1 \\ j\neq k}}^{K} \mathbf{s}_j y_{m,j}(i)\right] \\
&= \mathbf{w}_k^T(i)\left[\mathbf{r}(i) - \sum_{j=1}^{K} \mathbf{s}_j y_{m,j}(i)\right] + y_{m,k}(i)
\end{aligned} \tag{3.10}
$$

where $\mathbf{w}_k(i)$ is the blind adaptive MMOE detector given by (3.5) and this result follows from the fact that $\mathbf{s}_k$ is orthogonal to $\mathbf{x}_k$ and has unit energy. Using vector notation, we then have

$$
\mathbf{y}_{m+1}(i) = \mathbf{W}^T(i)\left[\mathbf{r}(i) - \mathbf{S}\mathbf{y}_m(i)\right] + \mathbf{y}_m(i) \tag{3.11}
$$

where $\mathbf{W}(i) = [\mathbf{w}_1(i), \mathbf{w}_2(i), ..., \mathbf{w}_K(i)]$. Now, using the recursion (3.11) and setting $\mathbf{y}_0 = 0$, we can express the soft decision output for an n-stage MMOE-PIC as $\mathbf{y}_n(i) = \mathbf{G}_n^T(i)\mathbf{r}(i)$, where

$$
\mathbf{G}_n^T(i) = \sum_{m=1}^{n} \left(\mathbf{I} - \mathbf{W}^T(i)\,\mathbf{S}\right)^{(m-1)} \mathbf{W}^T(i). \tag{3.12}
$$

Since $\mathbf{G}_n^T(i)$ represents a linear filter, the noise component in $\mathbf{y}_n(i)$ is still Gaussian

but with correlation matrix

$$E\left[\mathbf{G}_n^T(i)\mathbf{n}\mathbf{n}^T\mathbf{G}_n(i)\right] = \sigma_n^2\mathbf{G}_n^T(i)\mathbf{G}_n(i). \tag{3.13}$$

Thus, the BER performance of any user at any stage can be analytically calculated in the same way as for the matched filter detector [13]. Specifically, for binary phase-shift keying (BPSK) modulation, the conditional BER of user k at the ith symbol interval and stage n is given by

$$P_{n,k}[error|\mathbf{b}(i)] = Q\left\{\frac{\mathbf{g}_{n,k}^T(i)\mathbf{SAb}(i)}{\sigma_n\|\mathbf{g}_{n,k}\|}\right\} \tag{3.14}$$

where $\mathbf{g}_{n,k}(i)$ is the kth column of $\mathbf{G}_n(i)$.

3.2.3 BER Approximation

In AWGN channels with BPSK modulation, the kth user's average BER for the proposed receiver at stage n is obtained by averaging (3.14) over all possible interfering symbol combinations. Also note that for the adaptive receiver, the linear filter $\mathbf{g}_{n,k}(i)$ is not fixed but is a part of averaging. This implies that its performance can not be analyzed, so instead we take a Gaussian approximation approach to evaluate the BER performance for the proposed adaptive receiver.

For both the MMSE and the MMOE detectors, the residual interference can often be well modelled as a Gaussian random variable of appropriate variance [35].

Therefore, the BER can then be approximated by

$$P_e \cong Q(\sqrt{SIR}) \tag{3.15}$$

where SIR denotes signal to interference ratio (SIR). Note that the adaptive filter converges to the optimum filter tap weights in (3.4) as the number of iterations goes to infinity. Thus, if the adaptive filter misadjustment is low enough, we can express the conditional error probability for a given realization at steady-state as

$$P_{n,k}\left[error|\mathbf{b}\left(i\right)\right] \cong Q\left[\sqrt{SIR(i)}\right] \tag{3.16}$$

where

$$SIR(i) = \frac{\left[\mathbf{g}_{n,k}^{T}(i)\mathbf{s}_k\right]^2}{\left[\mathbf{g}_{n,k}^{T}(i)(\mathbf{r}\left(i\right) - b_k(i)\mathbf{s}_k)\right]^2}. \tag{3.17}$$

Averaging (3.17) over a number of realizations of the data vector $\mathbf{b}$, we get

$$SIR_{av} = \frac{\sum_{i=P}^{M}\left[\mathbf{g}_{n,k}^{T}(i)\mathbf{s}_k\right]^2}{\sum_{i=P}^{M}\left[\mathbf{g}_{n,k}^{T}(i)(\mathbf{r}\left(i\right) - b_k(i)\mathbf{s}_k)\right]^2} \tag{3.18}$$

where M and P indicate the start and end of the averaging process, respectively. In order to evaluate the steady-state BER performance, the averaged SIR needs to be computed after convergence is reached. Using (3.18), the average BER of the adaptive

receiver is then given by

$$P_{e,av}(n,k) \cong Q\left(\sqrt{SIR_{av}}\right). \tag{3.19}$$

This BER evaluation technique can be viewed as a hybrid of the Gaussian approximation and computer simulations. There is no general rule to determine the number of required averages. We study this in details in the following section.

3.2.4 Simulation Results

In this section we present simulation results for the systems discussed in the previous section. First, we present the convergence properties of the proposed algorithm. Then, we check the accuracy of the Gaussian approximation for the proposed adaptive detector in AWGN channels. The BER performance at steady-state is investigated at last. All simulation results are obtained in a near-far environment where the interfering users have a 20 dB higher energy than the desired user.

The convergence behavior of the multistage adaptive MMOE-PIC algorithm is shown in Figure 3.3. As can be seen from this figure, the adaptive LMS MMOE receiver requires approximately 800 training symbols before convergence can be reached. On the other hand, the RLS algorithm drives the SIR to 15dB in less than 400 symbols, which is roughly two times faster than the convergence time of the stochastic gradient algorithm. When it comes to the MMOE-PIC algorithm, a single iteration can drive the SIR to 15dB in less than 100 symbols. With more iterations, as shown in

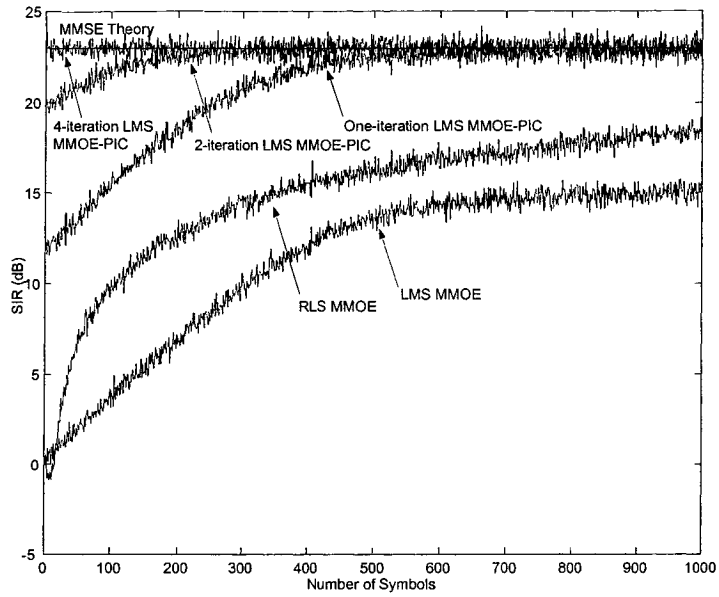

Figure 3.3: Averaged SIR versus time for the adaptive MMOE-PIC receiver compared to the conventional adaptive MMOE receiver for a synchronous 10-user DS-CDMA system with E_b/N_0=20dB, and N=31 (Gold Codes).

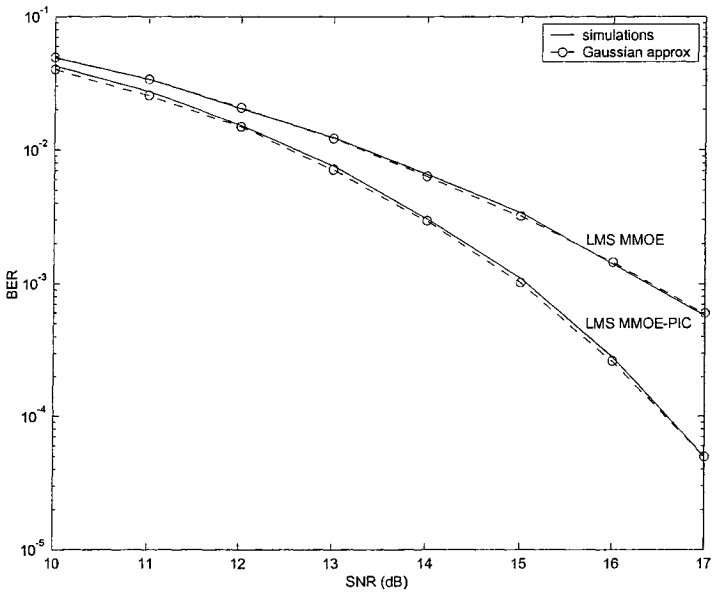

Figure 3.4: BER computed using Gaussian approximation and BER obtained by computer simulations of the adaptive MMOE-PIC receiver and the adaptive MMOE receiver versus SNR per symbol, K=20 users, and N=31 (Random Codes).

the plot, the proposed algorithm can further increase the convergence speed. Specifically, for the above DS-CDMA system, 4-iteration MMOE-PIC algorithm attains the MMSE theoretical SIR without training requirement. This is in contrast with the weighted linear PIC in [50] where it was shown that for a K-user system, K PIC stages and optimal choice of weights are required to achieve the MMSE theoretical SIR at the final stage. Thus, we can conclude that the proposed adaptive MMOE-PIC receiver is capable of providing near MMSE performance with less computational complexity than the weighted linear PIC which approaches the MMSE detector. Also note that the proposed receiver with different number of iterations attains the same steady-state SIR. It is therefore reasonable to assume that they achieve the same steady-state BER performance. Hence only the performance of a 1-iteration adaptive MMOE-PIC receiver is given for BER performance comparisons throughout following simulations.

The accuracy of the BER approximation presented in Section 3.2.3 is illustrated in Figure 3.4. Both computer simulations and approximate BER evaluation averaging over 10000 randomly chosen data sequences are performed. Spreading codes assigned to each user are randomly selected from a uniform distribution. The results in Figure 3.4 show that the Gaussian approximation yields a precise BER approximation for both the adaptive MMOE-PIC and the conventional adaptive MMOE receivers.

Finally, we investigate the steady-state BER performance for the proposed algorithm and its conventional counterpart in a severe near-far situation. These results are shown in Figure 3.5 and 3.6 using a long training period for both algorithms to

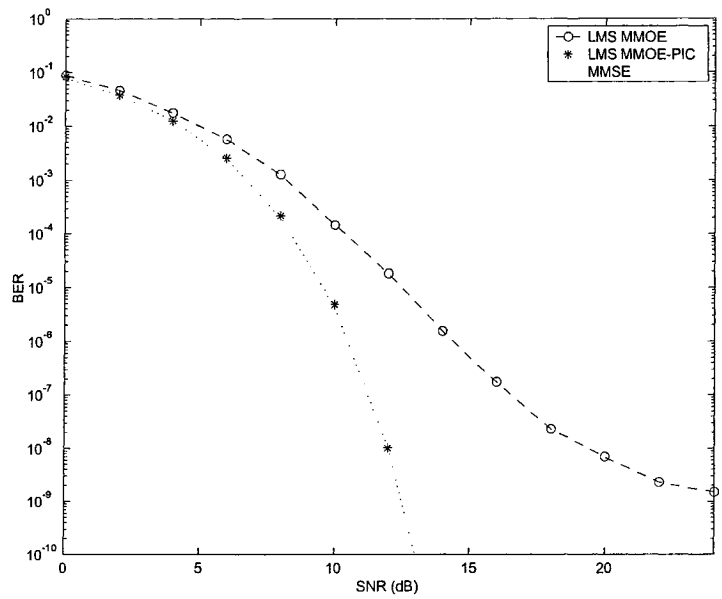

Figure 3.5: BER of the adaptive MMOE receiver and the adaptive MMOE-PIC receiver versus SNR per symbol, with K=10 users and N=31 (Gold Codes).

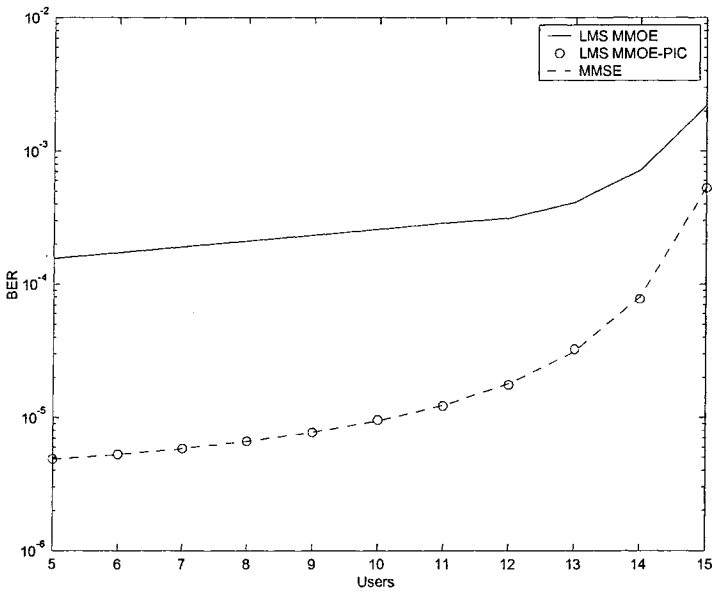

Figure 3.6: BER of the adaptive MMOE receiver and the adaptive MMOE-PIC receiver versus users with E_b/N_0=10dB and N=15 (Gold Codes).

ensure convergence. The BER analysis method is based on the Gaussian approximation presented in Section 3.2.3. The MMSE theoretical BER in (3.5) is also plotted for comparisons. As shown, the proposed adaptive algorithm achieves a BER performance which coincides with the theoretical LMMSE BER curve. On the other hand, the BER of the conventional adaptive MMOE detector shows an error floor at high SNR's due to the severe near-far problem which results in the imperfect filter coefficients. Note that the BER performance of the proposed receiver is excellent even at high SNR's and no error floor occurs. This superior performance is due to the fact that the decisions are correct with a high probability and the adaptive MMOE-PIC receiver can gain from that in terms of MAI estimation, whereas the conventional blind adaptive receiver suffers from a large performance loss due to the convergence problem in the severe near-far environment.

In Figure 3.6, we use short spreading sequences to observe the performance of both the MMOE and the MMOE-PIC algorithms in terms of the number of users. As shown, the proposed adaptive receiver can provide significant capacity gain over its conventional counterpart. For example, if we set the maximum tolerable BER to 2×10^{-4}, then the adaptive MMOE receiver is seen to accommodate 7 users whereas the proposed receiver can support 14 users. This represents a factor of 2 increase in user-capacity. It is also shown that the proposed adaptive MMOE-PIC receiver yields an identical performance with the optimum LMMSE detector even at high system loads.

3.3 Blind Adaptive MMOE-PIC in Asynchronous Channels

In this section, we derive the MMOE-PIC algorithm in asynchronous CDMA channels. The detection problem in asynchronous channels is more complicated than in synchronous channels. In a synchronous channel, by definition in Chapter 2, the bits of each user are aligned in time. Thus, detection can focus on one bit interval independent of the others, i,e., the detection of N bits of K users is equivalent to N separate "one-shot" detection problem. In most realistic applications, however, the channel is asynchronous and thus, there is overlap between bits of different intervals. Here, any decision made on a particular bit ideally needs to take into account the decisions on the 2 overlapping bits of each user. The decisions on these overlapping bits must then further take into account decisions on bits that overlap them and so on. Therefore, the MMOE-PIC receiver for synchronous channels must be modified and generalized to asynchronous channels by considering the 2 overlapping bits of each user in interference cancellation.

The rest of this section is organized as follows. First, an asynchronous DS-CDMA system model is described based on the synchronous channel model in Chapter 2. Then, we derive the proposed MMOE-PIC algorithm in asynchronous AWGN channels. The performance of the proposed detector in asynchronous AWGN channels is given finally.

3.3.1 Asynchronous System Model

The continuous-time model expressed in (2.3) can easily be generalized to asynchronous channel by including the relative time delays (offsets) between signals. The received signal is now written as

$$r(t) = \sum_{i=-\infty}^{\infty} \sum_{k=1}^{K} A_k b_k(i)\, s_k(t - iT - \tau_k) + n(t) \tag{3.20}$$

where τ_k is the delay of the kth user. Without loss of generality, τ_k is taken to be uniformly distributed over $[0, T)$. The received continuous-time signal is assumed to be sampled after front-end filtering and the receiver is synchronized to the desired user timing. Thus, the received signal vector for the ith symbol of the kth user is

$$\mathbf{r}_k(i) = \sum_{j=-P}^{P} \tilde{\mathbf{S}}_k(i-j)\mathbf{A}\mathbf{b}(i-j) + \mathbf{n}(i) \in \mathsf{R}^N \tag{3.21}$$

where $\tilde{\mathbf{S}}_k(i) = [\tilde{\mathbf{s}}_1(i), \tilde{\mathbf{s}}_2(i), ...\tilde{\mathbf{s}}_K(i)]$ is the sampled spreading sequence matrix with $\tilde{\mathbf{s}}_v(i)$ as the column vector of chip matched filter outputs (synchronized to the kth user) during symbol i associated with the inputs $s_v(t - iT - \tau_v)$. P denotes the channel spread. In particular, $P = 1$ for single path AWGN channels in this chapter.

3.3.2 Adaptive MMOE-PIC Algorithm in Asynchronous Channels

The blind adaptive MMOE-PIC detector for asynchronous CDMA systems has the same structure as shown in Figure 3.1. By taking into account the channel spread due to the transmission delay among users, we now generalize the proposed MMOE-PIC algorithm in Section 3.2.2 to asynchronous channels. Based on (3.21), the output vector for the kth user in the ith symbol interval and the $(m+1)$th cancellation stage can be written as

$$\mathbf{r}_{[PIC]m+1,k}(i) = \mathbf{r}_k(i) - \sum_{j=-P}^{P} \tilde{\mathbf{S}}_k(i-j)\Omega_{m,k}(i-j)\mathbf{y}_m(i-j). \tag{3.22}$$

Using the PIC algorithm, the discrete output signal $y_{m+1,k}(i)$ at the $(m+1)$th IC stage is then given by

$$\begin{aligned} y_{m+1,k}(i) &= \mathbf{w}_k^T(i)\mathbf{r}_{[PIC]m+1,k}(i) \\ &= \mathbf{w}_k^T(i)\left[\mathbf{r}_k(i) - \sum_{\substack{v=1 \\ v\neq k}}^{K} \tilde{\mathbf{s}}_v(i)y_{m,v}(i) - \sum_{\substack{j=-P \\ j\neq 0}}^{P}\sum_{v=1}^{K} \tilde{\mathbf{s}}_v(i-j)y_{m,v}(i-j)\right] \\ &= \mathbf{w}_k^T(i)\left[\mathbf{r}_k(i) - \sum_{j=-P}^{P}\sum_{v=1}^{K} \tilde{\mathbf{s}}_v(i-j)y_{m,v}(i-j)\right] + y_{m,k}(i) \end{aligned} \tag{3.23}$$

where $\mathbf{w}_k(i)$ is given by (3.5), and $\mathbf{s}_k$ is orthogonal to $\mathbf{x}_k$ with unit energy.

It is easy to show that the implementation complexity of the MMOE-PIC algorithm, given by (3.23), requires $O[10KNM + 2KN^2 + 4KN]$ flops where M is the

number of PIC iterations. On the other hand, the computational complexity of the optimum MMSE multiuser detector requires $O[11N_tK^3 + 6N_tK^2]$ flops where N_t is the finite memory length of the detector [73]. As can be observed, the complexity of the MMOE-PIC algorithm increases linearly with the number of users whereas the MMSE multiuser detector has a cubic dependence. At the same time, our results show that the MMOE-PIC can still perform close to the optimum MMSE detector. Other related work on the complexity of the MMSE multiuser detector and possible simple implementations include the work in [76].

It is important to mention that in our work we assume a perfect knowledge of all users' code sequences, similar to the MMSE multiuser detector. This assumption is important since the MMOE is known to be sensitive to code sequence mismatch [46]. In scenarios where such a mismatch exists, one can use alternative adaptive algorithms such as the one introduced in [46]. The proposed linear constrained constant-modulus (LCCM), in [46], is shown to be robust against errors in timing and code sequence estimates.

3.3.3 Simulation Results

In this section, we present simulation results for both the conventional MMOE and the proposed MMOE-PIC algorithms. First, we examine the convergence properties of the proposed algorithm. Then, we check the accuracy of the Gaussian approximation for both the MMOE and the MMOE-PIC receivers. Finally, we examine the self recovery capability of the proposed MMOE-PIC algorithm. Unless otherwise mentioned, a

Gold sequence family of length 31 chips is used.

Output SINR

The convergence behavior of the adaptive MMOE-PIC algorithm is shown in Figure 3.7. In Figure 3.7(a), the received signal energies are the same, whereas in Figure 3.7(b) the near-far problem is considered. Specifically, we consider a severe near-far scenario where all interfering users are at 10 dB higher SNR than the desired user. As seen from Figure 3.7(a), the adaptive MMOE receiver requires approximately 800 training symbols before convergence can be reached. On the other hand, for the case of severe near-far problem more than 2000 training symbols are required for convergence to be reached. A close look at the performance of the MMOE-PIC algorithm shows that a small number of IC stages can be sufficient to bring the performance close to the ideal MMSE detector. Furthermore, the effect of increasing the number of IC stages on the convergence speed is evident from the results in Figure 3.7. Specifically, with more than 2 IC stages, the training period required by the proposed receiver is almost the same for both environments in Figure 3.7(a) and Figure 3.7(b). We also observed that the proposed MMOE-PIC algorithm can significantly reduce the long training overhead introduced in the near-far situation, and successfully drive the output SINR close to the MMSE theoretical value.

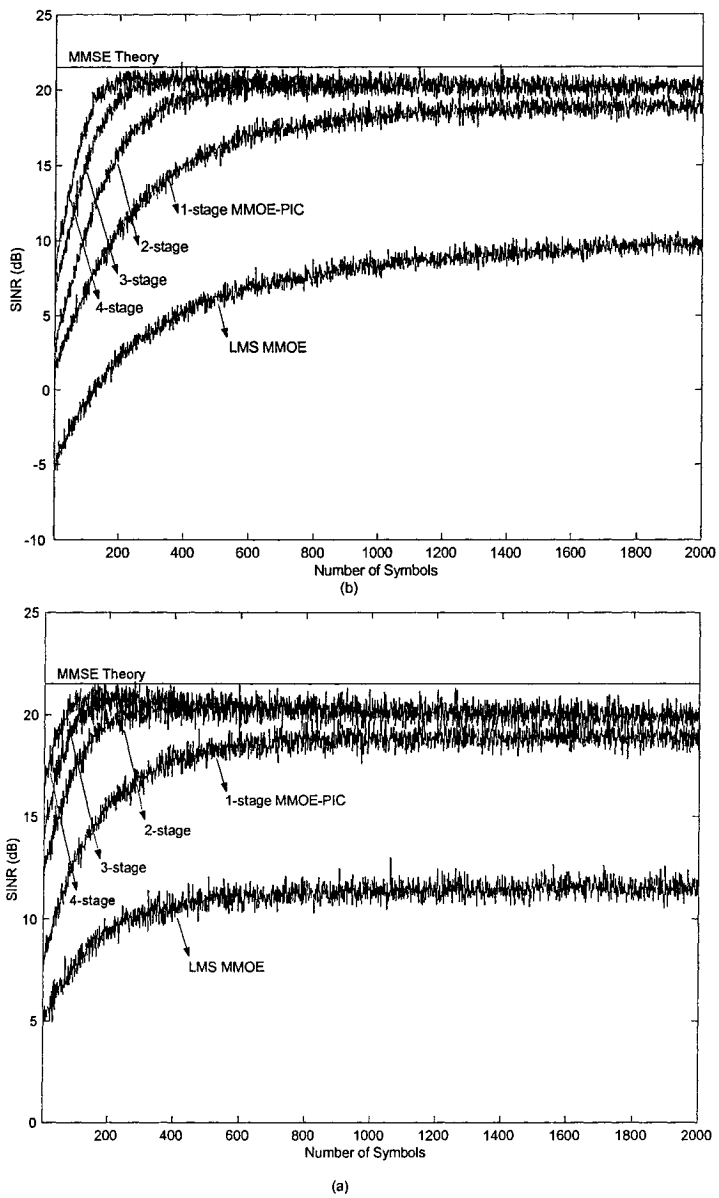

Figure 3.7: Averaged SINR of the adaptive MMOE-PIC receiver and the conventional adaptive MMOE receiver; $E_b/N_0 = 20$ dB, $K = 10$ users, $\mu = 10^{-1}$. (a) Equal received energies. (b) Near-far problem.

BER Performance and User-Capacity

In order to facilitate further discussions, the accuracy of the Gaussian approximation is first examined. Both computer simulations and the Gaussian approximation with an average taken over 10000 randomly selected data sequences are obtained. The results of this investigation are shown in Figure 3.8. In these results, we consider randomly selected spreading codes for all users. For the near-far scenario, the results show that the Gaussian approximation is accurate for both the adaptive MMOE and the proposed MMOE-PIC receivers. For the perfect power controlled scenario, we note that the Gaussian approximation becomes more accurate as the number of IC stages increases. It is also observed that at high SNR's, the Gaussian assumption yields a precise BER approximation evaluation for the adaptive MMOE-PIC receiver over both environments. Also since minimizing the MOE is equivalent to minimizing the MSE (equation (3.4)), one can expect that the performance of the MMOE receiver will converge to the decorrelator receiver at large SNR's.

Examining the performance of the MMOE-PIC versus the conventional MMOE receiver (see Figure 3.8), we see that the proposed receiver structure is more superior in both scenarios (equal power and near-far). It is shown that at high SNR's, the average BER of the adaptive MMOE receiver is significantly higher than the adaptive MMOE-PIC receiver. This poor performance of the standard adaptive MMOE receiver relative to the MMOE-PIC receiver is also clear from the attained SINR level at the end of the training period (see Figure 3.7).

Now, we investigate the BER performance versus SNR of the proposed algorithm

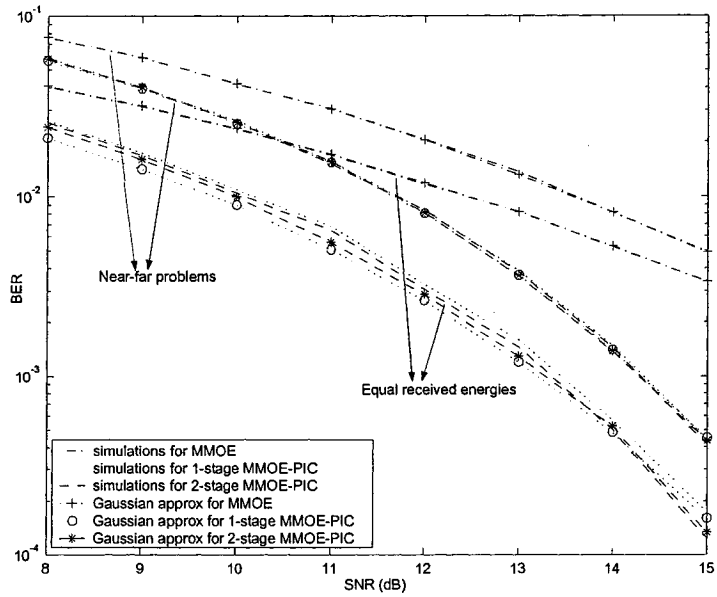

Figure 3.8: BER computed using the Gaussian approximation and BER obtained by computer simulations of the adaptive MMOE-PIC receiver and the adaptive MMOE receiver versus SNR per symbol; $K = 10$ users.

in Figure 3.9 where we consider Gold sequences and asynchronous transmission, and compare it with Figure 3.6 where synchronous channel is considered. Figure 3.9 and Figure 3.6 demonstrate that the proposed adaptive MMOE-PIC receivers degrade substantially in the presence of asynchronous transmission among users. This performance loss is mainly due to the combined effects of error propagation and imperfect coefficients. On the other hand, in asynchronous channels, the proposed MMOE-PIC detector still significantly outperforms the conventional adaptive MMOE receiver and achieves a BER performance which lies within 2 dB of the ideal LMMSE receiver at high SNR's.

In Figure 3.10, we plot the BER for both the MMOE and the MMOE-PIC algorithms as a function of the number of users. Also, we consider two scenarios: (1) equal

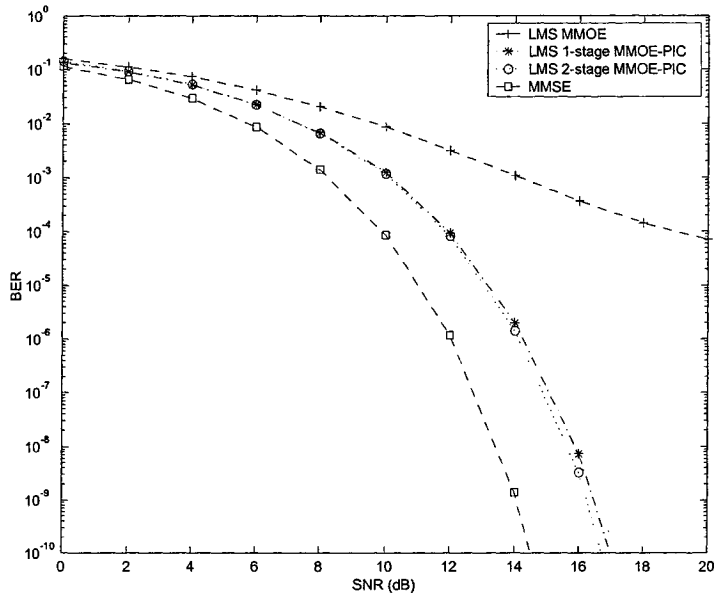

Figure 3.9: BER of the adaptive MMOE-PIC receiver and the adaptive MMOE receiver versus SNR per symbol; K=10 users, Near-far problem.

power users with SNR of 10 dB. (2) a near-far situation where the interfering users are at 10 dB SNR higher than the desired user. As shown, the proposed algorithm offers a significant increase in the number of users compared to the standard MMOE receiver. For instance, if the maximum tolerable BER is set to 2×10^{-3}, the adaptive MMOE receiver is shown to accommodate 4 users compared to 10 users for the proposed MMOE-PIC receiver in the near-far environment. This gain in user-capacity is more evident in the power-controlled scenario where the number of users can be increased to 13 users, more than a factor of 3 increase in system's user-capacity. These results also suggest that increasing the number of IC iterations can provide an increase in user-capacity for both equal power and near-far scenarios in systems with moderate loads.

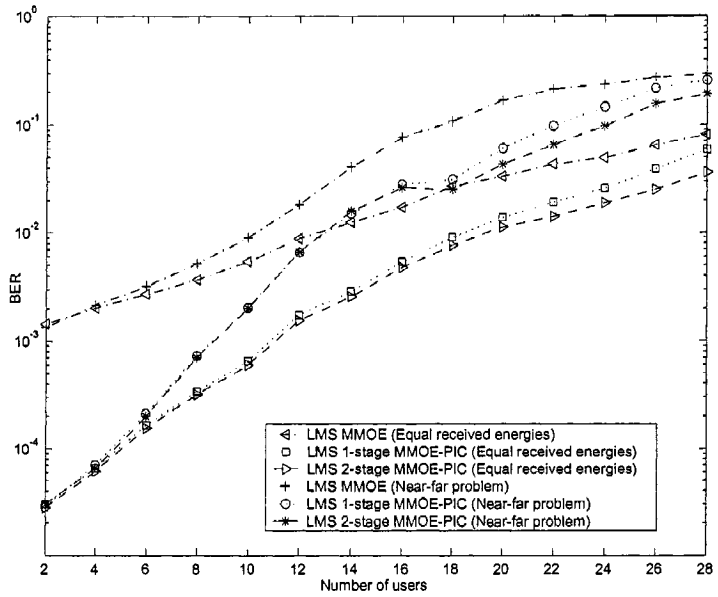

Figure 3.10: BER of the adaptive MMOE-PIC receiver and the adaptive MMOE receiver versus users; $E_b/N_0 = 10$ dB.

Self Recovery

Finally, in Figure 3.11, we examine the transient behavior of the MMOE-PIC algorithm due to abrupt changes in the number of interferers. The results in Figure 3.11 depict a scenario where a new user, with SNR larger than the desired user by 20 dB, is added to the system at iteration number 800. Our results show that both the MMOE and the MMOE-PIC have self recovery capabilities with varying degrees in sever near-far scenarios. One can see that the standard MMOE suffers from large SNR degradation of approximately 10 dB as opposed to one-stage MMOE-PIC where the SNR loss is more mild ranging from 5 dB. More interestingly, we observed that as the number of MMOE-PIC iterations increases the system becomes more robust

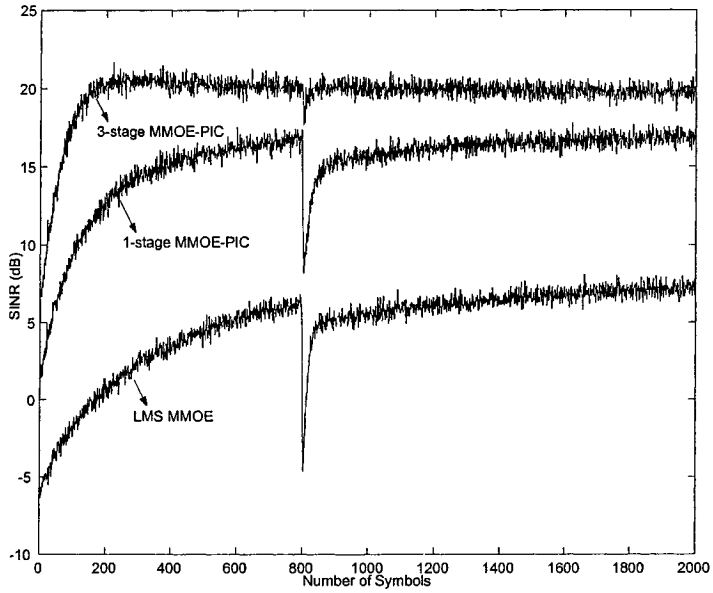

Figure 3.11: Averaged SINR of the adaptive MMOE-PIC receiver and the conventional adaptive MMOE receiver when a new user comes at the 800th iteration; $E_b/N_0 = 20$ dB, $K = 10$ users, $\mu = 10^{-1}$, Near-far problem.

to abrupt changes in the received signal amplitude. In fact, with 3 MMOE-PIC iterations both the recovery time and the instantaneous SNR degradation are shown to be minimal.

3.4 Conclusion

In this chapter, we introduced an adaptive MMOE-PIC iterative algorithm that is shown to effectively estimate users' signal amplitudes and hence, simplify the interference cancellation process. The proposed iterative algorithm offers much lower complexity than the MMSE multiuser detector with a comparable BER performance.

Further, we proved that the proposed receiver outperforms the conventional adaptive MMOE detector in-terms of the convergence speed and the BER achieved. We demonstrated that using only 1-stage MMOE-PIC detection scheme can sufficiently bring an identical performance to the ideal MMSE detector when synchronous transmission is considered. On the other hand, the proposed MMOE-PIC receiver was shown to experience performance degradation in asynchronous channels although it is still within 2 dB of the optimum LMMSE detection.

Chapter 4

Blind Adaptive LCMV-HD-PIC Detection in Dynamic Fading Channels

In chapter 2 various types of multiuser detection schemes as well as conventional detectors are reviewed. In Chapter 3 we introduced a new suboptimum multiuser detector, namely the blind adaptive MMOE-PIC detector, as well. We studied these detectors in AWGN channels. On the other hand, given the fact that CDMA transmissions are frequently made over channels that exhibit fading and /or dispersion, it would seem appropriate to design receivers for such channels. Henceforth we consider multiuser detection in dynamic fading channels.

In the present chapter, we propose an adaptive multistage detection scheme with

low complexity for DS-CDMA systems in the presence of time- and frequency- selective fading. The first stage is a blind adaptive multiuser detector based on the linear constrained minimum variance (LCMV) criterion. The interference cancellation occurs in the second stage. Our aim of this work is to study the performance of the proposed algorithm and investigate techniques for efficient multistage detection for CDMA systems in fading channels.

The rest of this chapter is organized as follows. In Section 4.1 previous related work on multiuser detection for fading channels is summarized and contribution of this chapter is described. Section 4.2 lays out the system model for the reverse link DS-CDMA in frequency-selective fading channels. In Section 4.3 we describe the proposed adaptive multistage detector which we choose for multiuser detection in fading channels. Section 4.4 presents simulation results of the proposed multiuser detector in both flat and frequency-selective fading channels. Finally, Section 4.5 concludes this chapter.

4.1 Introduction

4.1.1 Previous Work

In the past ten years multiuser detection theory has been extended to handle multiuser fading channels. Zvonar and Brady [51] have developed optimum detectors for slowly Rayleigh fading channels. They used a single-path fading model for the channel. In addition to the data detection, the received amplitude must be estimated in multipath

time-varying channels. Thus, the optimal multiuser receiver for fading channels is even more complex than the optimal receiver for AWGN channels. Previous work on slowly frequency-selective fading channels has been presented in [52]–[54]. Also, the optimal multiuser detector for very fast Rician fading channels has been presented in [55] and [56].

In order to relieve the prohibitive computational complexity of the optimal multiuser detector in fading channels, linear suboptimal decorrelating receivers for slowly fading channels have been considered in [53], [57], and [58]. The relatively fast fading channel case has been considered in [59], where decision-directed (DD) channel estimation was proposed. Furthermore, based on the more classical minimum mean-squared-error criterion, linear MMSE receivers for flat fading channels have been considered in [60]-[62]. Other related works on frequency-selective fading channels can be found in [63]-[65].

In additional to linear suboptimal detection, another class of nonlinear multistage detector was also generalized to multipath channels by Fawer and Aazhang in [66]. Nonlinear parallel interference cancellation receivers for slowly fading channels have been studied in [66, 70], and serial interference cancellation receivers in [67]. PIC receivers for relatively fast fading channels have been considered in [68] and [69].

4.1.2 Contribution

In this paper, we propose an adaptive multistage detection scheme where the first stage is the blind adaptive LCMV detector and the second stage is a PIC receiver.

The proposed receiver uses hard decision PIC on the standard least mean squares algorithm implementations of blind adaptive LCMV receiver to improve both the convergence rate and the BER performance in multipath fading channels. Therefore, it is also termed LCMV-HD-PIC receiver. Our aim of this work is to study the performance of the proposed algorithm and investigate techniques for efficient multistage detection for CDMA systems in fading channels. The simulation results show that the BER performance of the proposed algorithm approaches that of ideal detection without interference (single user bound) in flat fading channels even at high system loads. Moreover, it is observed through computer simulations that the proposed algorithm is insensitive to the number of users in flat fading channels. For multipath fading channels, from low to moderate SNR's, the performance of the proposed detector is within 1 dB of the single user bound at moderate system loads. However, the BER of the proposed receiver saturates at high SNR's since decision errors degrading the MAI estimates, especially in high loaded CDMA systems with near-far problem.

4.2 System and Channel Model

4.2.1 System Model

In mobile communication environments, since there are many propagation paths with different delays between the transmitter and the receiver, the transmitted signal components corresponding to these multipath propagation paths arrive at different times.

We assume a multiuser system in a multipath environment. The impulse response

of the channel for the kth user can be represented by a tapped delay line given by

$$h_k(t) = \sum_{l=1}^{L} c_{k,l}(t)\delta(t - \tau_{k,l}) \tag{4.1}$$

where $c_{k,l}(t)$ is the complex channel gain and $\tau_{k,l}$ is the delay of the lth path of the kth user. In this chapter, we assume that the path delays $\tau_{k,l} = lT_c$, $l = 1, ..., L$. Thus, the received baseband CDMA signal is the superposition of the channel distorted signals from the K users and the additive channel noise given by

$$\begin{aligned} r(t) &= \sum_{k=1}^{K} r_k(t) \otimes h_k(t) + z(t) \\ &= \sum_{i=0}^{N_b-1} \sum_{k=1}^{K} \sum_{l=1}^{L} A_k b_k(i) c_{k,l}(i) s_k(t - iT - \tau_k - \tau_{k,l}) + z(t) \end{aligned} \tag{4.2}$$

where $r_k(t)$ is the transmitted signal due to the kth user given by (3.20). $z(t)$ is the complex zero mean additive white Gaussian noise process with two-sided power spectral density σ_n^2, and $\otimes$ denotes convolution. The received signal in (4.2) is sampled at the output of the chip matched filter (CMF) at a rate of $T_c^{-1} = N/T$. Then, the received discrete-time signal $r(nT_c)$ can be expressed as

$$r(nT_c) = \sum_{i=0}^{N_b-1} \sum_{k=1}^{K} b_k(i) h_k[(n - \Delta\tau_k - iN)T_c] + z(nT_c) \tag{4.3}$$

$$h_k(nT_c) = \sum_{l=1}^{L} A_k c_{k,l}(i) s_k[(n - l)T_c] \tag{4.4}$$

where $h_k(t)$ is the composite signature waveform of user k, and $\Delta\tau_k$ is the delay of

user k in chip period T_c (we assume that τ_k is the integral times of T_c). Furthermore, notice that the composite signature vector of user k at symbol i can be decomposed to

$$\mathbf{h}_k(i) = A_k \mathbf{S}_k \mathbf{c}_k(i) \tag{4.5}$$

where

$$\mathbf{S}_k = \begin{bmatrix} p_k(0) & & 0 \\ \vdots & \ddots & p_k(0) \\ p_k(N-1) & & \vdots \\ 0 & \ddots & p_k(N-1) \end{bmatrix} \in \mathsf{R}^{(N+L-1)\times L}$$

$$\mathbf{c}_k(i) = [c_{k,1}(i), c_{k,2}(i), ..., c_{k,L}(i)]^T \in \mathsf{C}^{\mathsf{L}}. \tag{4.6}$$

Let us collect $N+L-1$ samples of $r(nT_c)$ in a vector $\mathbf{r}$. If the receiver is synchronized to the kth user, the vector $\mathbf{r}_k(i)$ has the expression

$$\mathbf{r}_k(i) = \sum_{j=-P}^{P} \tilde{\mathbf{H}}_k(i-j)\mathbf{b}(i-j) + \mathbf{z}(i) \in \mathsf{C}^{N+L-1} \tag{4.7}$$

where $\tilde{\mathbf{H}}_k(i) = [\tilde{\mathbf{h}}_1(i), \tilde{\mathbf{h}}_2(i), ...\tilde{\mathbf{h}}_K(i)]$ is the sampled composite spreading sequence matrix with $\tilde{\mathbf{h}}_v(i)$ as the column vector of chip matched filter outputs (synchronized to the user k) during symbol i associated with the inputs $h_v(t - iT - \tau_k)$.

$\mathbf{b}(i) = [b_1(i), b_2(i), ..., b_K(i)]^T$ is the data vector, and $\mathbf{z}(i)$ is the vector of noise samples at time i, assumed to be white with covariance $\sigma_n^2\mathbf{I}$.

4.2.2 Fading Channel Model

Channel coefficient vector $\mathbf{c} = [\mathbf{c}^T(0), \mathbf{c}^T(1), ..., \mathbf{c}^T(N_b-1)]^T$ where $\mathbf{c}(i) = [\mathbf{c}_1^T(i), \mathbf{c}_2^T(i), ..., \mathbf{c}_K^T(i)]^T$ is assumed to be a complex Gaussian random vector with zero mean and covariance matrix $\sum_{\mathbf{c}}$. It is assumed that the fading channel coefficients are complex Gaussian random variables with zero mean and variance normalized for convenience so that $\sum_{l=1}^{L}(|c_{k,l}(i)|^2) = 1$. The channel coefficients are assumed to be independent, i.e., $E\left(c_{k,l}(i), c^*_{k^0,l^0}(i)\right) = \sigma^2_{c_{k,l}}\delta_{k,k^0}\delta_{l,l^0}$, where δ_{k,k^0} is the discrete Kronecker delta function and $\sigma^2_{c_{k,l}} = E(|c_{k,l}(i)|^2)$ is the power of the lth path of user k. This assumption is equivalent to the common uncorrelated scattering (US) model [25]. The channels are assumed to be stationary over the observation interval so that the channel autocorrelation (autocovariance) function $\varphi_{k,l}(i, i^0) = E\left(c_{k,l}(i), c^*_{k,l}(i^0)\right)$ is a function of the time difference $i - i^0$ only. This assumption is equivalent to the common wide-sense stationary (WSS) model [32]. The stationary assumption is valid if the vehicle speed does not change during the transmission. The Doppler power spectrum is assumed to be the classical Jakes' spectrum ([71], Sec. 5.4), which results in the Clarke's channel autocorrelation function $\varphi_{k,l}(i) = \sigma^2_{c_{k,l}} J_0(2\pi f_d T i)$, where J_0 is the zero-order Bessel function of the first kind, $f_d = (v/C_{light})\, f_c$ is the maximum Doppler spread, v is the speed of the vehicle, c_{light} is the speed of light, and f_c is the carrier frequency.

4.3 Adaptive LCMV-HD-PIC Algorithm

In this section, we first introduce the blind adaptive LCMV algorithm for frequency-selective fading channels. Then, we propose a new multistage detector with LCMV in the first stage. The proposed algorithm exploits both the simplicity of the adaptive LCMV detector and the novelty of the multistage detector.

4.3.1 Blind Adaptive LCMV Detection for Multipath Channels

In Section 3.2.1 we studied the linear constraint optimization problem in the absence of multipath in which case the linear constraint is given by $\mathbf{w}^T\mathbf{s} = 1$. Unfortunately, constrained optimization methods are known to be very sensitive to signature mismatch due to signal cancellation effects [44]. Hence, special care needs to be taken when multipath is present. Following the similar ideas of Section 3.2.1, the receiver vector $\mathbf{w}_k(i)$ may be optimized by minimizing the output variance

$$\Im = E\left[\|y_k(i)\|^2\right] = \mathbf{w}_k^H(i)\Gamma_k(i)\mathbf{w}_k(i) \text{ and } \Gamma_k(i) = E\left[\mathbf{r}_k(i)\mathbf{r}_k^H(i)\right] \tag{4.8}$$

subject to the constraint that the response of the user of the interest is a constant

$$\mathbf{w}_k^H(i)\mathbf{h}_k(i) = 1 \tag{4.9}$$

where $\mathbf{h}_k(i)$ is the composite signature vector of user k and is priori known, and the superscript H represents Hermitian transpose operation. For a given $\mathbf{h}_k(i)$, this linear constraint minimum variance criterion results in the solution

$$\mathbf{w}_k(i) = \frac{1}{\mathbf{h}_k^H(i)\Gamma_k^{-1}(i)\mathbf{h}_k(i)}\Gamma_k^{-1}(i)\mathbf{h}_k(i) \tag{4.10}$$

where $\Gamma_k(i) = E[\mathbf{r}_k(i)\mathbf{r}_k^H(i)] = \sum_{j=-P}^{P}\sum_{k=1}^{K}\tilde{\mathbf{h}}_k(i-j)\tilde{\mathbf{h}}_k^H(i-j) + \sigma_n^2\mathbf{I}$, and the theoretical minimum mean-output-energy is given by

$$MMOE = \frac{1}{\mathbf{h}_k^H(i)\Gamma_k^{-1}(i)\mathbf{h}_k(i)} \tag{4.11}$$

It is shown in Section 3.2.1 and [44] that any $\mathbf{w}$ satisfying the constraint (4.9) can be represented in the canonical form as

$$\mathbf{w}_k(i)=\alpha_k(i)\mathbf{h}_k(i) + \mathbf{x}_k(i) \text{ where } \mathbf{h}_k^H(i)\mathbf{x}_k(i) = 0 \tag{4.12}$$

where $\alpha_k(i)\mathbf{h}_k(i)$ is the nonadaptive part and $\alpha_k(i)$ is a scalar which makes the weight vector $\mathbf{w}_k(i)$ satisfy the constraint (4.9). $\mathbf{x}_k(i)$ is the adaptive part which lies in the nonspace of $\mathbf{h}_k(i)$.

In order to minimize output variance with respect to $\mathbf{x}_k(i)$, the gradient of output variance in (4.8) is given by

$$\nabla_{\mathbf{x}}(MOE) = 2P_{\mathbf{h}}^{\perp}\mathbf{R}_k(i)\mathbf{w}_k(i) = 2[\mathbf{I} - \mathbf{h}_k(i)\mathbf{h}_k^H(i)]\Gamma_k(i)\mathbf{w}_k(i) \tag{4.13}$$

where $P_{\mathbf{h}}^{\perp} = [\mathbf{I} - \mathbf{h_k}(i)\mathbf{h}_k^H(i)]$ represents the subspace orthogonal to $\mathbf{h_k}(i)$. Finally, by using an instantaneous approximation $\hat{\Gamma}_k(i) = \mathbf{r}_k(i)\mathbf{r}_k^H(i)$ for $\Gamma_k(i)$, the stochastic gradient adaptation rule is given by

$$\mathbf{x}_k(i+1) = \mathbf{x}_k(i) - \mu[\mathbf{I} - \mathbf{h}_k(i)\mathbf{h}_k^H(i)]\mathbf{r}_k(i)y_k(i) \tag{4.14}$$

where μ is the step-size parameter and $y_k(i) = \mathbf{w}_k^T(i)\,\mathbf{r}_k(i)$ is the output of the blind adaptive detector.

4.3.2 Blind Adaptive LCMV-HD-PIC Algorithm

Suboptimum multiuser detection based on interference cancellation from tentative decisions was introduced in the form of multistage detection by Varanasi and Aazhang [12]. The two-stage detector makes a decision at the second stage on a user's symbol by estimating and then subtracting from that user's matched filter output. The choice of the first stage proved to be important in the performance of the multistage detector [13]. Particularly, the multistage detector based on decorrelating first stage was shown to perform significantly better than the decorrelating detector, in a number of situation of practical interest such as in high bandwidth utilities and near-far situations [13]. On the other hand, it was shown in [73] that in the time-varying channels, an ideal computation of the decorrelating or the LMMSE detector requires $O[cN_f(KL)^3]$ flops where N_f is the frame length and c is a constant depending on the algorithm. The implementation complexity has cubic dependence on KL, and is too

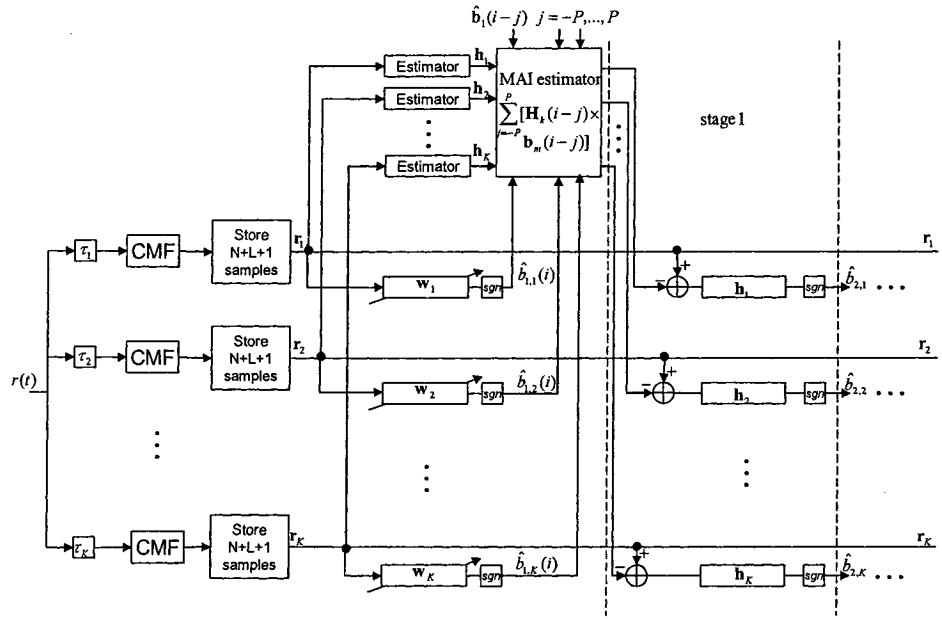

Figure 4.1: LCMV-HD-PIC receiver for multipath fading channels

high for several practical implementations. Clearly, we need simpler implementations of linear MUD to replace the decorrelating detector as the first stage of multistage detection in a dynamic CDMA system.

Motivated by the above thought, we propose an adaptive multistage PIC structure where we employ the blind adaptive LCMV algorithm as the base decision function in the first stage. The proposed receiver structure is depicted in Figure 4.1. As shown, the interference suppression is performed using a multistage nonlinear PIC with the hard decisions obtained from the blind adaptive LCMV multiuser detector.

The output of adaptive LCMV detector and the corresponding tentative decisions are

$$y_{[LCMV],k}(i) = \mathbf{w}_k^H(i)\mathbf{r}_k(i) \tag{4.15}$$

$$\hat{b}_k(i) = sgn\left\{\mathrm{Re}\left[y_{[LCMV],k}(i)\right]\right\} \tag{4.16}$$

The interference suppression performs multistage PIC utilizing hard decisions. The output vector for the kth user at the ith symbol interval and the mth cancellation stage is given by

$$\mathbf{r}_{[PIC],m,k}(i) = \mathbf{r}_k(i) - \sum_{j=-P}^{P} \tilde{\mathbf{H}}_k(i-j)\Omega_{m,k}(i-j)\hat{\mathbf{b}}_m(i-j) \tag{4.17}$$

where $\Omega_{m,k}(i-j) \in [0,1]^{K\times K}$ is a diagonal matrix including the weights for partial interference cancellation. The weight for the ith symbol of desired user is set to zero (i.e., $\gamma_{m,k}(i) = 0$). On the other hand, the weights $\gamma_{m,k^0}(i^0) \in [0,1]$ for user $k^0 \neq k$ and $i^0 \neq i$ depend on the estimated quality of the decision statistic for the corresponding user. Here, however, a constant weight $\gamma_{m,k^0}(i^0) = 1$ is used throughout the cancellation process. Using the PIC algorithm, the discrete output signal at the

mth IC stage is given by

$$
\begin{aligned}
y_{[PIC],m,k}(i) &= \mathbf{h}_k^H(i)\mathbf{r}_{[PIC]m,k}(i) \\
&= \mathbf{h}_k^H(i)\left[\mathbf{r}_k(i) - \sum_{\substack{v=1 \\ v\neq k}}^{K} \tilde{\mathbf{h}}_v(i)\hat{b}_{m,v}(i) - \sum_{\substack{j=-P \\ j\neq 0}}^{P}\sum_{v=1}^{K} \tilde{\mathbf{h}}_v(i-j)\hat{b}_{m,v}(i-j)\right] \\
&= \mathbf{h}_k^H(i)\left[\mathbf{r}_k(i) - \sum_{j=-P}^{P}\sum_{v=1}^{K} \tilde{\mathbf{h}}_v(i-j)\hat{b}_{m,v}(i-j)\right] + \hat{b}_{m,k}(i)\mathbf{h}_k^H(i)\mathbf{h}_k(i).
\end{aligned}
\tag{4.18}
$$

Using vector notation, we can write the output of the LCMV-HD-PIC receiver as

$$
\mathbf{y}_{[PIC],m}(i) = \mathbf{y}(i) - \sum_{j=-P}^{P} (\mathbf{R}(i-j) - \boldsymbol{\delta}_{j,0}\Psi(i))\hat{\mathbf{b}}_m(i-j) \tag{4.19}
$$

where $\mathbf{y}(i)$ is the output of the bank of matched filters. $\mathbf{R}(i)$ is the correlation matrix, and $\Psi(i)$ is a diagonal matrix with the diagonal element $\mathbf{h}_k^H(i)\mathbf{h}_k(i)$. The output vector of the tentative decision is then obtained as

$$
\hat{\mathbf{b}}_{m+1}(i) = sgn\left\{\mathrm{Re}\left[\mathbf{y}_{[PIC],m}(i)\right]\right\}. \tag{4.20}
$$

4.4 Simulation Results

Here, the performance of the proposed LCMV-HD-PIC detector is investigated by Monte-Carlo computer simulations, since the proposed receiver is highly nonlinear and its performance can not be analyzed. Both flat and frequency-selective fading

channels are considered. In particular, the frequency-selective channel for each user consists of three independent Rayleigh fading paths separated by T_c. The delay of the users is assumed to be uniformly distributed over $[0, T)$ .The Doppler power spectrum is assumed to follow Jakes' model [75] with vehicle speed 60 km/h, carrier frequency 2 GHz, and symbol rate 16 kbits/s. A Gold sequence family with processing gain 31 is used in the simulations. The BER simulations are carried out in steady-state after a training period of 5000 symbols. The simulation results are obtained by averaging the BER's of randomly selected users with different delays. Simulations include examples with equal transmitted energies for all users, and examples with a near-far problem.

The BER performance of the proposed adaptive LCMV–HD-PIC algorithm in flat fading channels is shown in Figure 4.2 and 4.3 where both moderate ($K = 20$) and heavy ($K = 30$) system loads are considered. In Figure 4.2(a) and Figure 4.3(a), the received signal energies are the same for all active users, whereas in Figure 4.2(b) and Figure 4.3(b) the near-far problem is considered. Specifically, we consider a severe near-far scenario where all the interfering users have a 10 dB SNR higher than the desired user. In Figure 4.2, the BER performance of the LCMV-HD-PIC algorithm demonstrates that a small number of interference cancellation (IC) stages yield performance close to the ideal detection without interference. The similar performance can be observed in Figure 4.3 where a heavy loaded system ($K = 30$) is considered. Moreover, it can be observed form Figure 4.3 that conventional blind adaptive LCMV receiver and the first stage of the proposed detector become interference limited in heavy loaded systems with a near-far problem. On the other hand, the BER curves

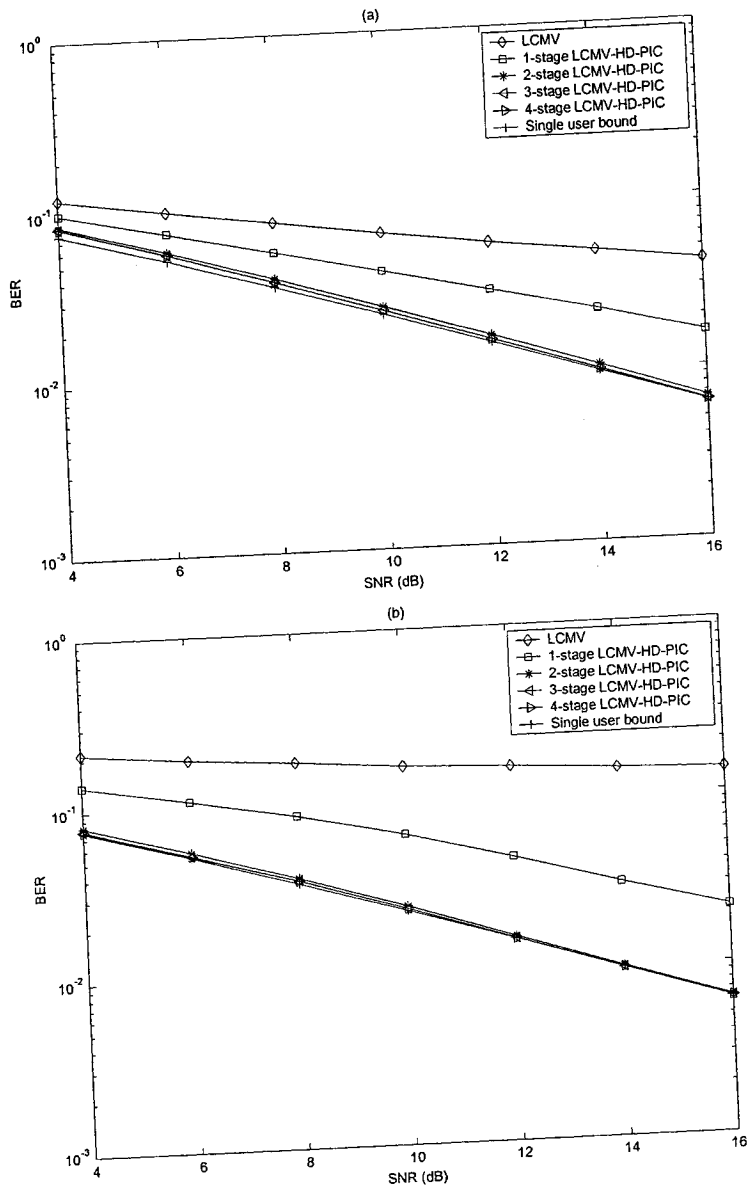

Figure 4.2: BER performance of the LCMV-HD-PIC receiver versus SNR in a flat fading channel; K=20 users. (a) Equal received energies. (b) Near-far problem.

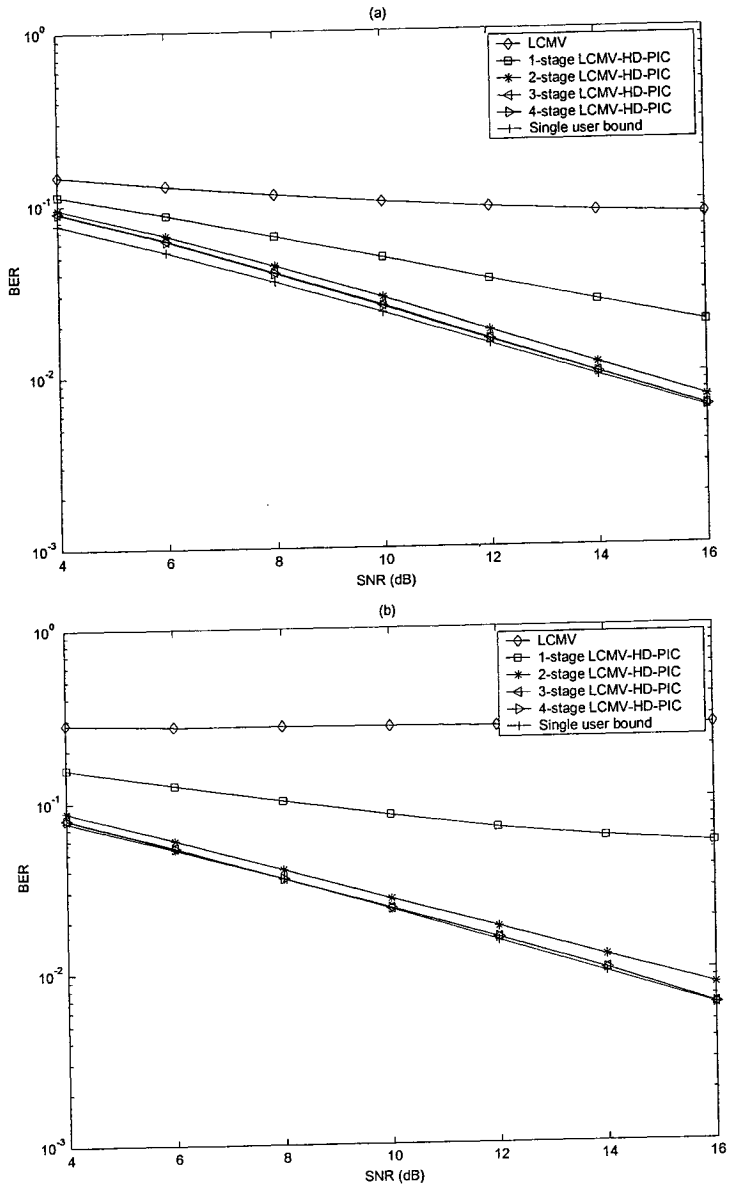

Figure 4.3: BER performance of the LCMV-HD-PIC receiver versus SNR in a flat fading channel; K=30 users. (a) Equal received energies. (b) Near-far problem.

of the third and fourth stage of the LCMV-HD-PIC detector approach that of the single user bound at high SNR's.

Figure 4.4 shows plots of BER performance for the proposed adaptive LCMV-HD-PIC receiver versus the number of users in flat fading channels. It can be observed that the performance of the proposed detector is not sensitive to the number of users. Figure 4.4(a) shows that the third stage and fourth stage of the LCMV-HD-PIC detector can achieve a performance which is very close the single user bound. On the other hand, Figure 4.4(b) demonstrates that the BER curve of a 3-stage LCMV-HD-PIC receiver coincides with the single user bound, meaning that three stage is enough for the adaptive LCMV-HD-PIC to achieve the optimum performance even in heavy loaded systems with a severe near-far problem. Moreover, the second stage of the proposed receiver suffers from a small performance degradation relative to the single user bound in both scenarios.

Now, we investigate the BER performance versus SNR for the proposed algorithm and its conventional counterpart in frequency selective fading channels. These results are shown in Figure 4.5 where simulations are performed only for $K = 20$ active users to simplify the simulations. Both cases of equal received energies and a near-far problem are considered. It is shown that from low to moderate SNR's, a 4-stage LCMV-HD-PIC lies within 1 dB (in SNR) of ideal detection in the absence of interference. However, the BER of the LCMV-HD-PIC receiver saturates at high SNR's since decision errors degrade the MAI estimates, especially in the systems with near-far problem. It is also observed that the performance difference between

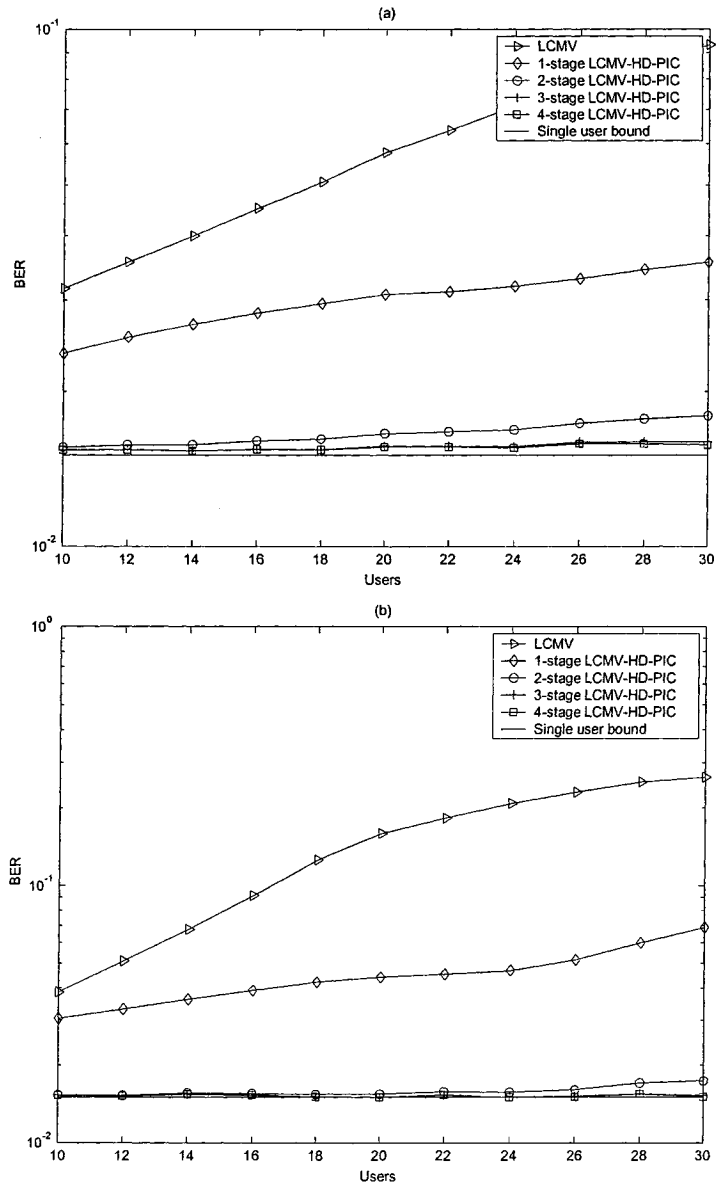

Figure 4.4: BER performance of the LCMV-HD-PIC receiver as a function of the number of users in a flat fading channel; SNR=12 dB. (a) Equal received energies. (b) Near-far problem.

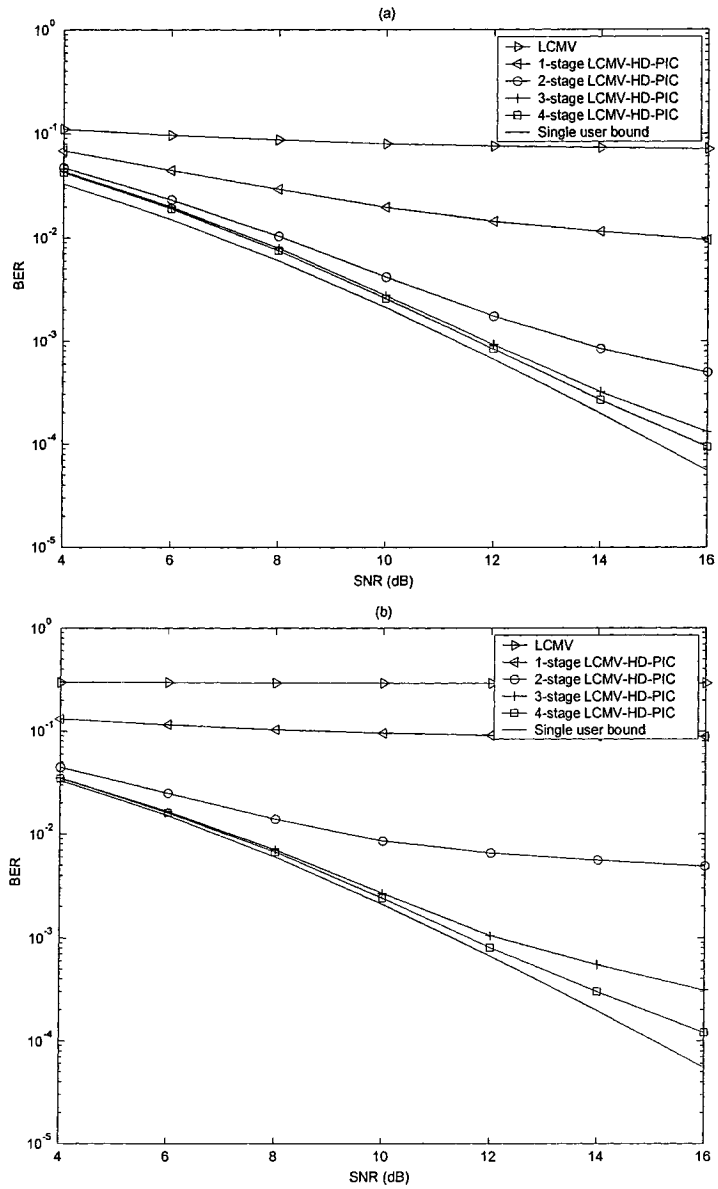

Figure 4.5: BER performance of the LCMV-HD-PIC receiver versus SNR in a frequency-selective channel (L=3); K=20 users. (a) Equal received energies. (b) Near-far problem.

the third stage and fourth stage is negligible from low to moderate SNR's whereas at high SNR's the performance gap becomes larger since the BER of the third stage saturates earlier than the fourth stage as the SNR increases. It can be concluded that the proposed LCMV-HD-PIC detector with more than 3 stages suffers less than 1 dB relative to the single user bound and can provide satisfactory performance at most practical system loads and SNR's. On the other hand, the proposed receiver suffers from BER saturation at high SNR's due to the error propagation, which can be effectively relieved by increasing the number of IC stages.

In Figure 4.6, we plot the BER of the adaptive LCMV-HD-PIC algorithm as a function of the number of users in frequency-selective channels. We observe that the performance of the proposed LCMV-HD-PIC detector is more sensitive to the system loads in frequency-selective channels than flat fading channels. In particular, a 4-stage LCMV-HD-PIC receiver can achieve same performance over different number of users from low to moderate system loads. On the other hand, the proposed receivers degrade substantially in highly loaded systems. Moreover, the results in Figure 4.6(b) show that the degradation is more severe in systems with a near-far problem. We also observe that the third stage of the LCMV-HD-PIC algorithm offers a significant increase in user-capacity relative to the second stage. For instance, if we set the maximum tolerable BER to 1×10^{-3}, a 3-stage LCMV-HD-PIC receiver can accommodate 19 users as opposed to 10 users for a 2-stage LCMV-HD-PIC receiver in the near-far environment. This user-capacity gain is seen to increase to 10 users for systems with perfect power control, which represents a factor of 2 increase in

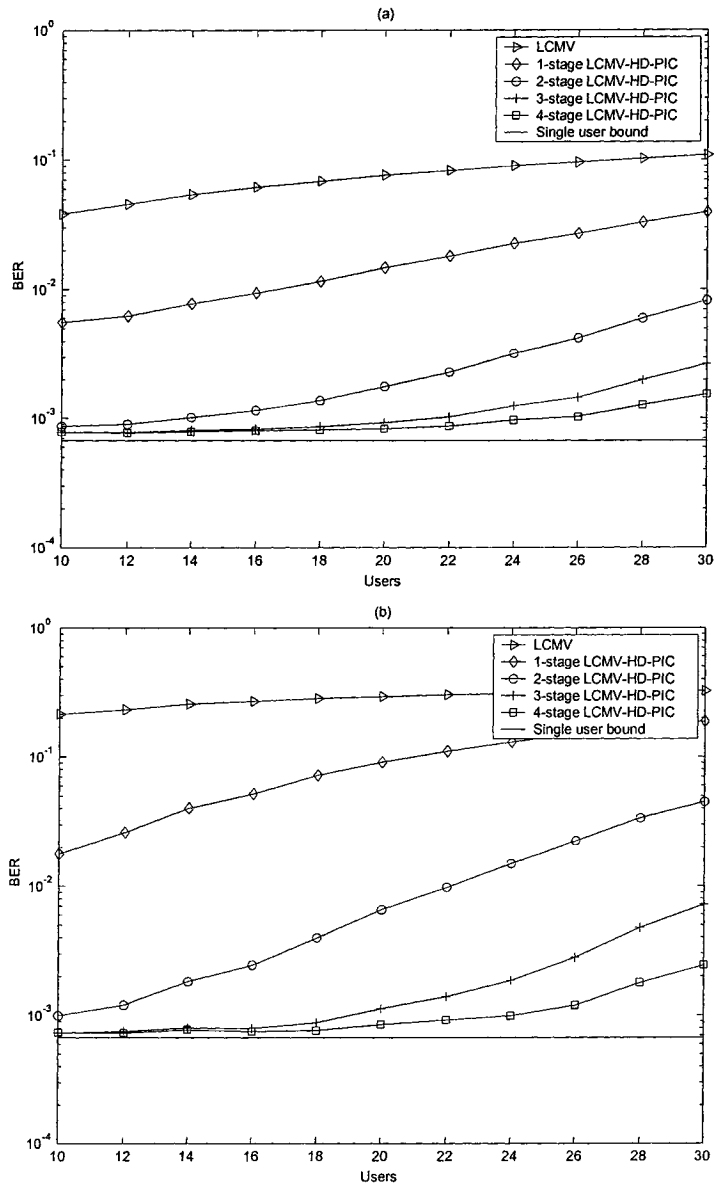

Figure 4.6: BER performance of the LCMV-HD-PIC receiver as a function of the number of users in a frequency-selective channel (L=3); SNR=12 dB. (a) Equal received energies. (b) Near-far problem.

user-capacity. On the contrary, the performance difference between the third stage and the fourth stage is negligible from low to moderate system loads. At high system loads, the fourth stage gradually outperforms the third stage, but the performance gain is not significant. This result also demonstrates that increasing the number of IC stages provides increase in user-capacity for heavily loaded systems.

4.5 Conclusion

In this chapter, we introduced an adaptive multistage LCMV-HD-PIC algorithm whose first stage is an blind adaptive LCMV detector followed by IC stages. In flat fading channels, it was shown that a 3-stage LCMV-HD-PIC can achieve a performance which is very close to the single user bound and insensitive to the system loads. In frequency-selective fading channels, the proposed algorithm was shown to offer an excellent performance complexity tradeoff since it is within 1dB of ideal detection at moderate SNR's and system loads. It was also shown that in frequency-selective channels, the BER performance of the proposed detector degrades significantly at high system loads and increasing the number of IC stages can relieve this performance degradation.

Chapter 5

Adaptive Nonlinear MMSE-DFD in Fast-Fading Channels

In Chapter 4, a blind adaptive multistage detector was proposed and shown to offer near-optimum performance at practical SNR's and system loads over both flat and frequency-selective fading channels. However, the ability of our blind adaptive multiuser detector to successfully combat multiuser interference is based on the exact knowledge of the signature waveform of each user. In the fading channels, however, the transmitted waveforms are subject to unknown (and time-varying) channel distortion. Therefore, it is important to obtain an adaptive multiuser detector which can provide a tradeoff between performance and complexity in practical fading channels without the knowledge of user's spreading sequence. In this chapter, we propose a multistage decision feedback multiuser detector based on successive interference cancellation for fast fading channels. The proposed multiuser detector employs a

modified adaptive LMMSE algorithm as the feed-forward detector and only needs training data sequences for every active user for initial adaptation.

The chapter is organized as follows. In Section 5.1 previous related literature is reviewed and the contributions of this chapter are put into perspective. In Section 5.2 we briefly describe the system that we consider in this chapter. Section 5.3 gives the derivation of the proposed decision feedback multiuser detector for fast fading channels. In Section 5.4 we present simulation results of the proposed detector in both flat and frequency-selective fast fading channels. Finally, Section 5.5 concludes the chapter.

5.1 Introduction

5.1.1 Previous Work

Linear minimum mean-squared-error detection has been proposed as an alternative to the matched filter receiver for DS-CDMA systems (see [26, Ch. 6] and [90] and references therein). In particular, given a training sequence, the adaptive LMMSE receiver does not require explicit estimates of the interference parameters such as relative amplitudes, phases, and spreading codes for initial adaptation. On the other hand, the use of standard adaptive interference suppression algorithms in time varying channels may result in poor performance results. For instance, in [61] a severe tracking problem has been reported when a conventional MMSE adaptive receiver was used in a frequency-nonselective (flat) fading channel. It was shown that the standard

LMMSE adaptive algorithm can lose track of the time varying channel when the channel goes into a deep fade. In addition to this, adaptive MMSE receivers are known to breakdown if the time variations of the channel are too fast relative to the transmission rate [77]. To solve these channel tracking problems, several modified adaptive algorithms have been proposed in [60]-[62] for flat fading channels, and in [63]-[65] and [77] for frequency-selective fading channels. For an excellent literature survey of the different MMSE adaptive algorithms, the reader is referred to [78] and [79].

In multipath fading channels, the decentralized algorithms often suffer from imperfect filter adaptation due to: large system loads, severe near-far problems, and/or large levels of intersymbol interference (ISI) [80]. To overcome these problems, researchers have recently focused on a class of nonlinear decision feedback MUD techniques [16], [17] and [81]-[85] (and references therein). Initial work on decision-feedback detection was first introduced in [16]. The proposed nonlinear feedback receiver in [16] uses previous and/or tentative decisions of data at the output of the feedback filter to cancel the effects of multiple access interference (assuming no errors in the feedback direction). More recent works related to nonlinear detection include the work in [81] where a class of MMSE multiuser DFDs (MMSE-DFDs) was proposed. These DFDs are relatively simple to implement and their performance is shown to be significantly better than linear MMSE multiuser detectors over AWGN channels. The adaptation for both the feed-forward and the multiuser feedback filters in [81] is jointly optimized in a MMSE sense using a training sequence. Similar to

the work in [19], but including adaptive antennas, [84] has proposed a space-time adaptive MMSE decision-feedback multiuser detector for high data rate applications over quasi-static frequency-selective fading channels. Up to this point, and to the best of our knowledge, all the works dealing with MMSE-DFD and its adaptive implementation have assumed either an AWGN channel model [81], [83], [85] or a slowly time-varying multipath fading channel [84].

5.1.2 Contribution

In this chapter we extend the work of [81] to frequency-selective fast-fading channels. It is assumed that the channel parameters for all users are perfectly known at the receiver. The modified MMSE-DFD receiver has less adaptation requirements than the adaptive MMSE-DFD in [84], and is suitable for fast fading channels. The proposed receiver incorporates the complex channel coefficients in the adaptation process for both the feed-forward and feedback filters. In this case, the receiver employs a modified MMSE optimization function which results in a separate adaptive filter for each resolvable path. In fixed multipath channels, and using the modified (precombining) MMSE-DFD, our results show a minimal performance loss from the standard (post-combining) MMSE-DFD receiver (i.e., the one that employs DFD after multipath combining).

5.2 System Model

The system model that we study in this chapter is the same as the one we studied in Chapter 4. However, here we make different assumptions, which lead to different analysis. We consider a K-user asynchronous DS-CDMA system model where each user signal propagates through L different paths. The received signal has the form

$$r(t) = \sum_{i=0}^{N_b-1} \sum_{k=1}^{K} \sum_{l=1}^{L} A_{k,l} b_k(i) c_{k,l}(i) s_k(t - iT_s - \tau_{k,l}) + n(t) \tag{5.1}$$

where $A_{k,l}$, $b_k(i)$, $c_{k,l}(i)$, $s_k(t)$, and $\tau_{k,l}$ are the received amplitude, the ith transmitted BPSK modulated data symbol, the complex fading coefficient, the spreading sequence, and the relative delay for the lth received path, all for the kth user's signal, respectively. In (5.1), N_b is the number of the received symbols and $n(t)$ is the white Gaussian noise with two-sided power spectral density σ_n^2. We assume that the fading among different users is independently and identically distributed (iid). We also assume that all path delays $\tau_{k,l} < T_s$, where T_s is the symbol interval. Now, the lth path of the kth user's contribution to $r(t)$ is

$$r_{k,l}(t) = \sum_{i=-\infty}^{\infty} b_k(i) c_{k,l}(i) g_{k,l}(t - iT_s) \tag{5.2}$$

where

$$g_{k,l}(t) = A_{k,l} s_k(t - \tau_{k,l}). \tag{5.3}$$

The received signal, in (5.1), is applied to a chip matched filter and the output is sampled at a rate of $T_c^{-1} = N/T_s$. If we let $\mathbf{r}$ be the vector containing the samples over a data block of length N_b symbols, we can write

$$\mathbf{r} = \mathbf{SCb} + \mathbf{n} \in \mathbf{C}^{N_b N} \tag{5.4}$$

where the vector $\mathbf{r} = [\mathbf{r}^T(0), ..., \mathbf{r}^T(N_b-1)]^T$ with elements $\mathbf{r}^T(i) = [r(iT_s+T_c), ..., r(iT_s+NT_c)]$, $\mathbf{C} = diag[\mathbf{C}(0), ..., \mathbf{C}(N_b-1)] \in \mathbf{C}^{KLN_b \times KN_b}$ is the channel coefficient matrix with $\mathbf{C}(i) = diag[\mathbf{c}_1(i), ..., \mathbf{c}_K(i)] \in \mathbf{C}^{KL \times K}$ and $\mathbf{c}_k(i) = [c_{k,1}(i), c_{k,2}(i), ...c_{k,L}(i)]^T \in \mathbf{C}^L$, $\mathbf{b} = [\mathbf{b}^T(0), ..., \mathbf{b}^T(N_b-1)]^T \in \Xi^{KN_b}$ is the data vector with $\mathbf{b}^T(i) = [b_1(i), ..., b_K(i)]$, and $\mathbf{n} \in \mathbf{C}^{N_b N}$ represents the sampled noise vector. In (5.4), $\mathbf{S} = [\mathbf{S}(0), ...\mathbf{S}(0), ..., \mathbf{S}(N_b-1)] \in \mathbf{R}^{N_b N \times KLN_b}$ is the windowed signature sequence matrix with $\mathbf{S}(i) = [\mathbf{s}_{1,1}(i), \mathbf{s}_{1,2}(i), ..., \mathbf{s}_{K,L}(i)]$, and $\mathbf{s}_{k,l}(i)$ is the windowed signature for the symbol $b_k(i)$ and channel parameter $c_{k,l}(i)$, defined as

$$\mathbf{s}_{k,l}(i) = E(b_k^*(i)c_{k,l}^*(i)\mathbf{r}). \tag{5.5}$$

This windowed signature for a given symbol and channel coefficient represents the signature of the lth path of the kth user as seen through the receiver time span. Assuming uncorrelated data symbols and normalized complex fading coefficients (i.e., $E(|c_{k,l}|^2) = 1$), a direct calculation of the pth element, $s_{k,l}(p)$, of the windowed

signature $\mathbf{s}_{k,l}(i)$ yields to

$$\begin{aligned} s_{k,l}(p) &= E(b_k^*(i)c_{k,l}^*(i)r(pT_c)) \\ &= b_k^*(i)c_{k,l}^*(i)r_{k,l}(pT_c) \\ &= \sum_{i=-\infty}^{\infty} g_{k,l}(pT_c - iT_s) \end{aligned} \tag{5.6}$$

where $p = 1, ..., N_bN$, and * denotes complex conjugate operation.

5.3 Precombining MMSE-S-DFD

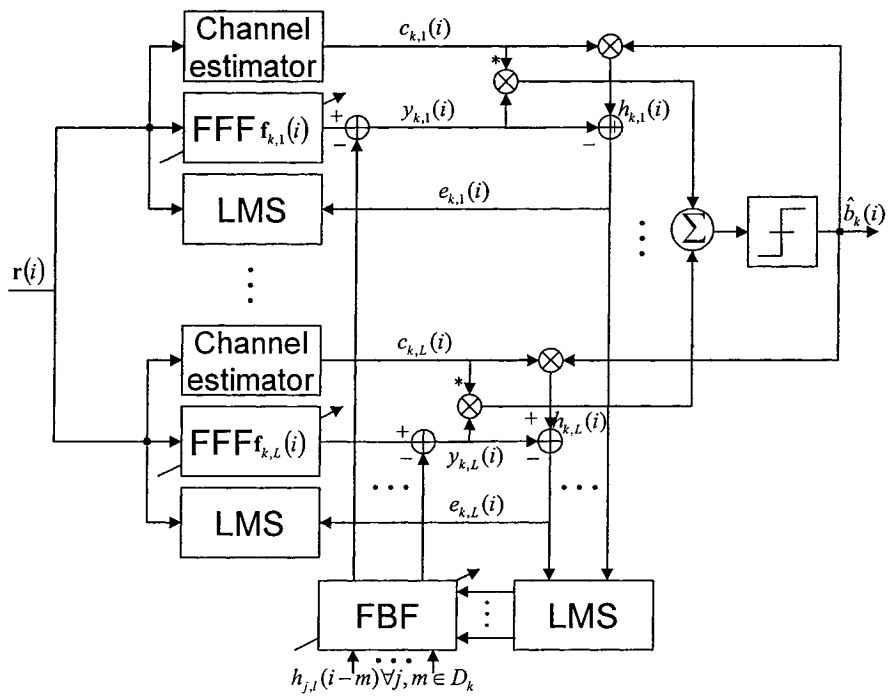

Figure 5.1: General block diagram of the precombining adaptive MMSE-S-DFD receiver.

The proposed receiver structure is shown in Figure 5.1. As shown, the feed-forward filter (FFF) processes N_f chip samples from a chip matched filter. It was shown in [30] that a multiuser finite-impulse response (FIR) filter of time span less than ten symbols is in many cases sufficient for practical detection of user data. In this chapter, the received signal is processed in blocks of M symbols where $M = 3$ symbols. Now if we let the input sample vector at the ith data bit be $\bar{\mathbf{r}}(i) = [\mathbf{r}^T(i - P), ...\mathbf{r}^T(i), ..., \mathbf{r}^T(i + P)]^T \in \mathsf{C}^{MN}$ with $M = (2P + 1)$, we can write

$$\bar{\mathbf{r}}(i) = \sum_{k=1}^{K} \sum_{m=-L_S}^{L_S} \mathbf{S}_k(i - m)\mathbf{c}_k(i - m)b_k(i - m) + \mathbf{n}(i) \tag{5.7}$$

where L_S represents the span of the channel time dispersion. We further define the FFF coefficients vector with impulse response $\mathbf{f}_{k,l}(i) = [f_{k,l}^{(0)}(i), ..., f_{k,l}^{(MN-1)}(i)]^T \in \mathsf{C}^{MN}$.

Similar to the structure of the FFF, the multiuser successive feedback filter (S-FBF) processes a finite number of the most recent N_s data symbols from all users and current data symbols from detected users. Instead of feeding back hard data decisions of $b_k(i)$ as in [84], we use as a reference signal the soft estimate $b_k(i)c_{k,l}(i)$ for the FBF contents. This approach can avoid the FBF from tracking the fading coefficients of all paths for all users, which are often too fast for typical adaptive algorithms to track. Assuming perfect channel state information (at the receiver) and correct data decisions $b_k(i)$ at the FBF output, the precombining MMSE-FBF will subtract the postcursor ISI and the MAI due to the previous symbols of all users

and current symbols of detected users. In order to diminish the detrimental effects of error propagation in DFDs, we consider successive DFDs which detect and feedback the current symbols of the users in a specified order as in [81]. Using the partition of users as in [81], the S-DFD divides the users into two groups

$$D_k = \left\{ \begin{array}{c} 1,...,K : m \in \{1,2,...,N_s\} \\ \\ 1,...,k-1 : m = 0 \end{array} \right\}$$

$$U_k = \{\bar{D}_k\} \tag{5.8}$$

where $m \in \{0,...,N_s\}$ represents the feedback symbol set. That is the most recent N_s data symbols from all users and current data symbols from detected users. Based on the partition in (5.8), and given a FBF with coefficients vector $\mathbf{w}_{k,l}(i)$, we define the feedback data vector

$$\mathbf{h}_k(i) = [h_{1,1}(i-N_s),...,h_{j,l}(i-m),...,h_{k-1,L}(i)]^T \in \mathbb{C}^{KLN_s+(k-1)L} \tag{5.9}$$

with $j \in D_k$, $m \in \{0,...,N_s\}$, and $h_{j,l}(i) = b_k(i)c_{k,l}(i)$. Now to find the optimum MMSE feed-forward and feedback filters' coefficients, we form two vectors

$$\mathbf{x}_k^H(i) = [\bar{\mathbf{r}}^H(i), \mathbf{h}_k^H(i)] \tag{5.10}$$

and

$$\mathbf{u}_{k,l}^H(i) = [\mathbf{f}_{k,l}^H(i), \mathbf{w}_{k,l}^H(i)]. \tag{5.11}$$

The output of the lth branch of the kth user can then be written as

$$y_{k,l}(i) = \mathbf{u}_{k,l}^H(i)\mathbf{x}_k(i) \tag{5.12}$$

and $y_{k,l}(i)$, $l = 1, .., L$ can then be combined coherently as shown in Figure 1.

Note that the only dependence of user j's coefficients on user i is through the reliability of user j's previous and current (if $j < i$) decisions that are fed back to user i. Throughout the steady-state analysis, we assume that all feedback decisions are correct. Also in order to remove the dependence of the FFF and FBF on the state of the fading channel, we choose $\mathbf{u}_{k,l}(i)$ to minimize the modified MSE criterion

$$MSE_{k,l}(\mathbf{u}_{k,l}) = E\left\{\left|b_k(i)c_{k,l}(i) - \mathbf{u}_{k,l}^H(i)\mathbf{x}_k(i)\right|^2\right\}. \tag{5.13}$$

The solution of this optimization problem is given by the Wiener-Hopf equation as

$$\mathbf{u}_{k,l}(i) = \mathbf{R}_k^{-1}(i)\mathbf{v}_{k,l}(i) \tag{5.14}$$

where

$$\mathbf{R}_k(i) = E\{\mathbf{x}_k(i)\mathbf{x}_k^H(i)\} \tag{5.15}$$

and

$$\mathbf{v}_{k,l}(i) = E\{\mathbf{x}_k(i)b_k^*(i)c_{k,l}^*(i)\} = \mathbf{s}_{k,l}(i). \tag{5.16}$$

The matrix $\mathbf{R}_k(i)$ can be written as

$$\begin{aligned}\mathbf{R}_k(i) &= E\{\mathbf{x}_k(i)\mathbf{x}_k^H(i)\} \\ &= E\left\{\begin{array}{cc} \mathbf{r}(i)\mathbf{r}^H(i) & \mathbf{r}(i)\mathbf{h}_k^H(i) \\ \mathbf{h}_k(i)\mathbf{r}^H(i) & \mathbf{h}_k(i)\mathbf{h}_k^H(i) \end{array}\right\} \\ &= \left\{\begin{array}{cc} \Upsilon(i) & \Theta_k(i) \\ \Theta_k^H(i) & \Phi_k(i) \end{array}\right\}.\end{aligned} \tag{5.17}$$

From (5.17), it is easy to show that

$$\Theta_k(i) = [\mathbf{S}_1(i), ...\mathbf{S}_j(i-m), ..., \mathbf{S}_K(i-N_s)]_{j\in D_k, m\in\{0,...,N_s\}} \tag{5.18}$$

and

$$\Upsilon(i) = \sum_{k=1}^{K}\sum_{m=-L_S}^{L_S} \mathbf{S}_k(i-m)\mathbf{S}_k^H(i-m) + \mathbf{R}_{nn} \tag{5.19}$$

where $\mathbf{R}_{nn} = E\{\mathbf{n}(i)\mathbf{n}^H(i)\}$ is the autocorrelation matrix corresponding to the FFF noise vector, and $\Phi_k(i) = \mathbf{I}$ where $\mathbf{I}$ is the identity matrix. Using (5.17)-(5.19), the FFF and the FBF coefficients are given by

$$\mathbf{f}_{k,l}(i) = \left\{ \sum_{j \notin D_k} \sum_{m=-L_S}^{L_S} \mathbf{S}_j(i-m)\mathbf{S}_j^H(i-m) + \mathbf{R}_{nn} \right\}^{-1} \mathbf{v}_{k,l}(i) \tag{5.20}$$

$$\mathbf{w}_{k,l}(i) = -\Theta_k^H(i)\mathbf{f}_{k,l}(i) \tag{5.21}$$

As discussed in [81], due to the partitioning of users, different users obtain different performance levels resulting in a non-uniform performance over all users. This is due to the structure of the decision feedback detector where only interference from the recent N_s symbols and all current symbols of all users in set D_k is cancelled using the FBF. The remaining interference from the rest of the users in set U_k is compensated by the feed-forward filter in MMSE sense. One solution to this non-uniform performance problem was suggested in [81] where a two-stage MMSE-S-DFD is used to successively detect users in a reverse order (relative to the first stage). In this case, the first stage is the same as before while the second stage uses soft data decisions at the output of the first S-DFD stage (shown in Figure 5.2). Based on this algorithm, users' data in the second stage are detected successively using the first stage stored decisions.

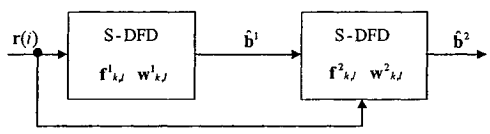

Figure 5.2: A 2-stage DFD with successive detection at each stage.

As opposed to the work in [81], where a centralized nonlinear S-DFD was proposed for time invariant channels, we introduced a modified precombining adaptive implementation of the 2-stage receiver suited for multipath fast-fading channels. To relax the tracking requirements of the MMSE feed-forward filter, the modified nonlinear decision feedback detector is employed prior to multipath maximal ratio combining. As it will be seen, shortly, the nonlinear structure of the modified receiver is robust against MAI, ISI, and the number of resolvable paths in the fast-fading channel.

Up to this point, we have only considered centralized multiuser detection where explicit knowledge of all users' parameters is needed at the receiver side. Since adaptive implementations are usually less computationally complex than centralized implementations, in what follows, we present a stochastic gradient algorithm for the nonlinear decision feedback detector. We rely on adaptive trained techniques where initial filter adaptation is achieved using a training sequence, after which the nonlinear receiver switches to the decision directed mode. Note that in both modes of operations (i.e., training and decision directed) the receiver uses a modified estimate for filter's adaptation incorporating both the detected data symbol and the corresponding channel coefficient associated with the desired user's resolvable path. From (5.13), the gradient of the modified MMSE function is given by

$$\nabla_{\mathbf{u}}(MSE) = 2(\mathbf{R}_k(i)\mathbf{u}_{k,l}(i) - \mathbf{v}_{k,l}(i)). \tag{5.22}$$

Using the normalized least-mean-squared algorithm, the coefficients of the nonlinear

receiver (both FFF and FBF) can simply be adjusted in an adaptive manner using the following recursion

$$\begin{aligned}\mathbf{u}_{k,l}(i+1) &= \mathbf{u}_{k,l}(i) - \lambda \bigtriangledown_{\mathbf{u}} (MSE) \\ &= \mathbf{u}_{k,l}(i) + 2\lambda[\tilde{h}_{k,l}(i) - \mathbf{u}_{k,l}^{H}(i)\mathbf{x}_k(i)]^{*}\mathbf{x}_k(i) \end{aligned} \tag{5.23}$$

where $\tilde{h}_{k,l}(i) = b_k(i)c_{k,l}(i)$ in the training mode, and λ is the time-variant step-size parameter chosen to reduce the effects of channel variations on the adaptation process [49].

5.4 Simulation Results

In this section, we present simulation results to investigate the performance of the modified MMSE-S-DFD receiver over both flat and frequency-selective fading channels. The simulation parameters used in our study are listed as follows (unless otherwise mentioned): carrier frequency at 2.0 GHz, symbol rate of 16 kbits/s, and 15-chip Gold codes. An asynchronous reverse link equal energy multipath Rayleigh fading channel is considered. The delay between two adjacent paths is a random variable uniformly distributed over the interval $[1, 6)$ chips. The fast-fading scenario corresponds to a mobile speed of 40km/h. In what follows, we refer to the proposed modified nonlinear receiver with successive feedback as the precombining MMSE-S-DFD, and we call its conventional counterpart (with standard MMSE optimization cost function) as the postcombining MMSE-S-DFD.

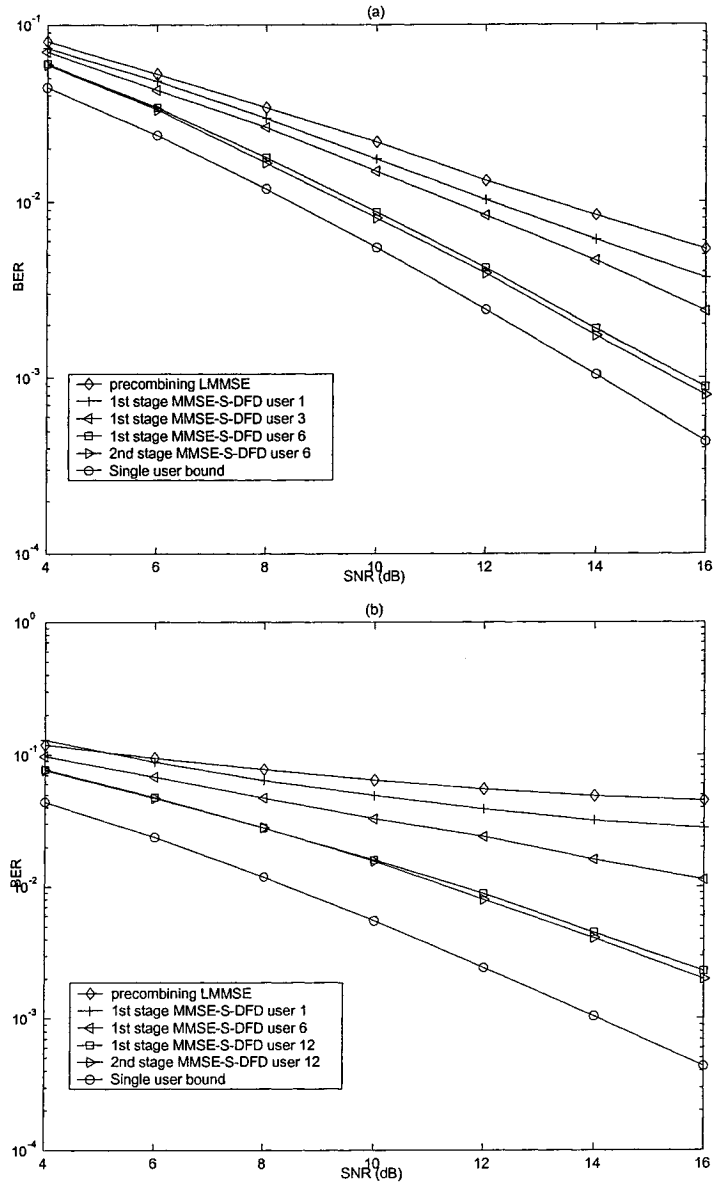

Figure 5.3: BER as a function of the averaged SNR for the precombining adaptive LMMSE receiver and the 2-stage precombining adaptive MMSE-S-DFD in a two-path fading channel. (a) 6 users; (b) 12 users.

5.4.1 Nonlinear Versus Linear Detection in Fast-Fading

Figure 5.3 compares the performance of the precombining adaptive LMMSE and the proposed 2-stage precombining adaptive MMSE-S-DFD using the adaptive algorithm in (5.23). These results are obtained for a 6-user (Figure 5.3.a) and 12-user systems (Figure 5.3.b). Four curves are shown for the proposed 2-stage MMSE-S-DFD, corresponding to the performance obtained for user 1, user $K/2$, the last user of the first stage, and the last user of the second stage, respectively. The performance results for the precombining LMMSE receiver corresponds to the results of the precombining LMMSE receiver presented in [77]. We see that the MMSE-S-DFD offers a significant performance improvement relative to the precombining MMSE receiver in the fast-fading channel. Note that, in the first stage, the last user receives the best performance due to the successive feedback detection. On the other hand, the first user of the MMSE-S-DFD (only) receives cancellation of the MAI and ISI from previous symbols. The advantage of this DFD is that it can be implemented in a parallel style, and hence avoiding multistage detection. Our results show that the performance of the first user (i.e., worst performance) at the first stage of the proposed receiver is still better than the performance of the linear receiver in both heavily and medium loaded systems. On the other hand, the second stage of the proposed MMSE-S-DFD offers significantly lower BER performance compared to both the precombining LMMSE and the one-stage MMSE-S-DFD. Specifically, the performance of the last user in the second stage of the precombining 2-stage adaptive MMSE-S-DFD is within 2 dB

of the ideal detection (single user bound) in a 6-user CDMA system. It is also observed that the performance difference between the last user in the first stage and the last user in the second stage is negligible which proves that the 2-stage adaptive MMSE-S-DFD offers nearly uniform performance over all users.

5.4.2 Flat Fading

Figure 5.4 deals with the difference in performance between the precombining adaptive LMMSE receiver and the proposed 2-stage precombining adaptive MMSE-S-DFD in flat Rayleigh fading channels. Both fast fading and slow fading scenarios are considered. For the slow-fading channel, we consider a mobile with 4km/h and the same parameters as before. We clearly see that the proposed adaptive MMSE-S-DFD offers no loss in performance from slow to fast fading channels, even when the system is heavily-loaded (see Figure 5.4.b). As a final observation, we see that the performance of the precombining MMSE-S-DFD in the flat fading case is closer to the single user bound than in the multipath channel (Figure 5.3).

5.4.3 Effect of Multipath

To examine the effect of multipath on the receiver performance, we increase the number of paths for all users to four resolvable paths. The results are shown in Figure 5.5 for the MMSE-S-DFD and the LMMSE over both fast and slow fading channels. In these results, we assume that all users's paths are of equal energy. Based on these results, we can draw the following conclusions:

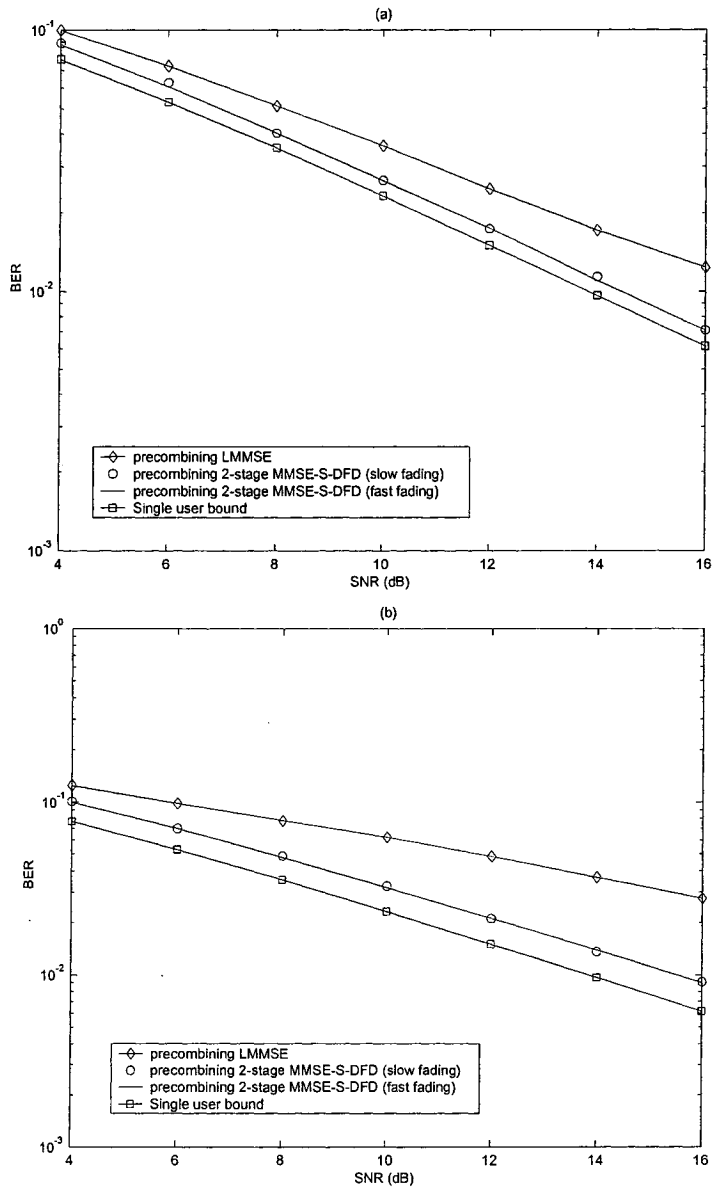

Figure 5.4: BER as a function of the averaged SNR for the precombining adaptive LMMSE receiver and the 2-stage precombining adaptive MMSE-S-DFD in fast and slow flat Rayleigh fading channels. (a) 6 users; (b) 12 users.

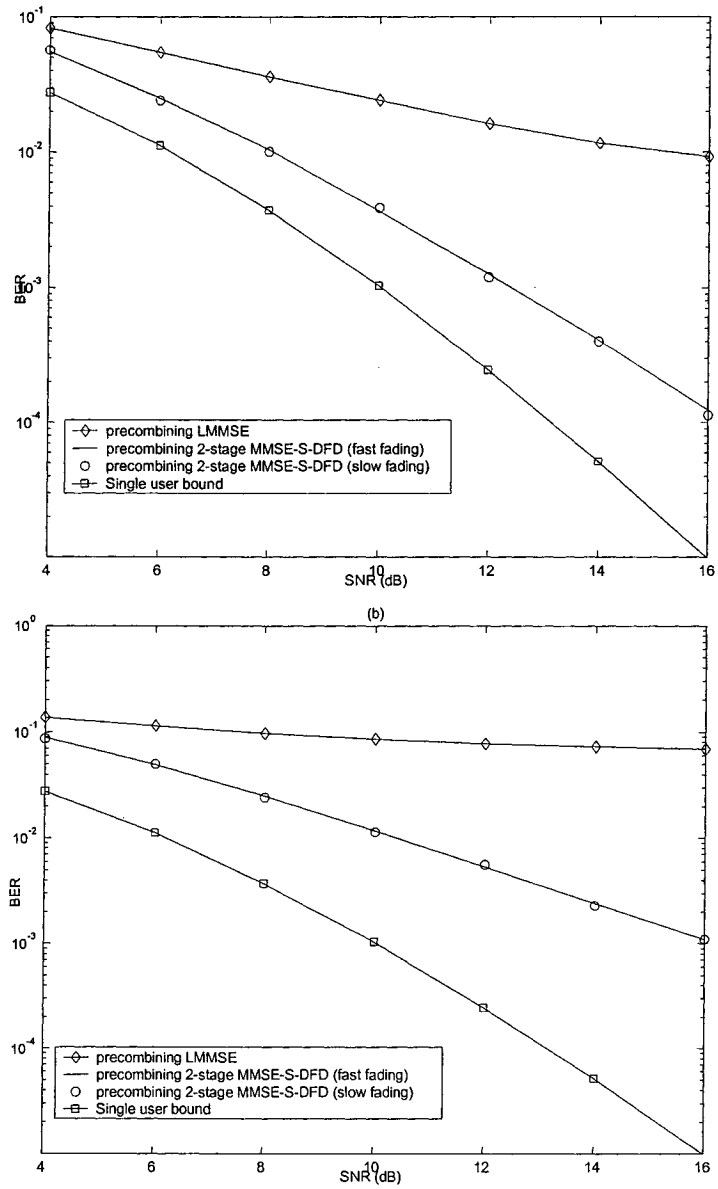

Figure 5.5: BER of the precombining adaptive LMMSE receiver and the 2-stage precombining adaptive MMSE-S-DFD in a four-path fading channel. (a) 6 users; (b) 12 users.

1. The performance of the precombining LMMSE receiver deteriorates as the number of paths increases. On the other hand, the proposed precombining MMSE-S-DFD provides much better performance (relative to the LMMSE) as the signal energy is distributed among more paths.

2. The MMSE-S-DFD performs the same over both fast and slow fading channels.

3. When the system load and the number of paths per user are both large, the precombining LMMSE receiver suffers from large performance degradation exhibited in the error floor shown in Figures. 5.3.b, 5.5.b. On the other hand, the MMSE-S-DFD is still able to contend to large interference levels but with a limited performance gain. One can use the same argument as in [78] to explain the performance difference between the LMMSE and the MMSE-S-DFD in heavily loaded multipath channels with large number of resolvable paths. Simply put, the use of multiuser feedback filtering in the MMSE-S-DFD helps to conserve the available degrees of freedom for the feed-forward filter. Hence a better interference rejection capability is supplied by the feed-forward filter relative to the LMMSE filter, which has to use its own degrees of freedom to cope with the overall input interference.

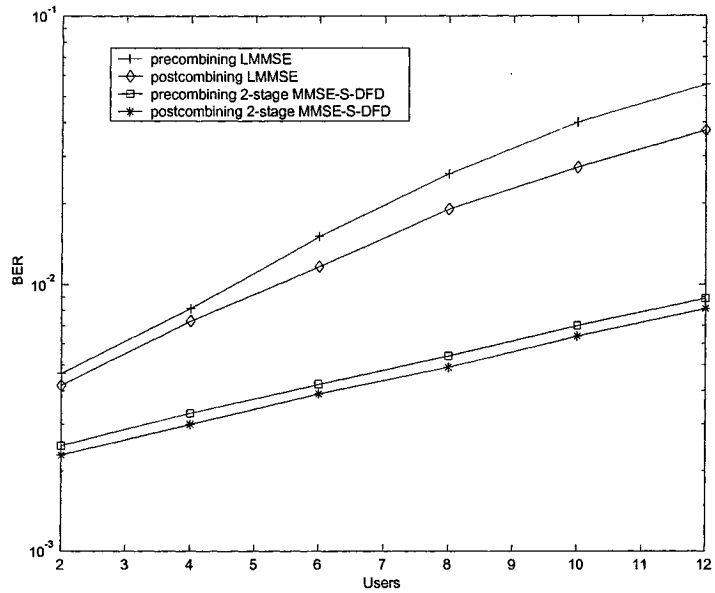

Figure 5.6: BER as a function of the number of users for the postcombining adaptive MMSE-S-DFD and the precombining adaptive MMSE-S-DFD in a fixed multipath channel with SNR=12 dB.

5.4.4 Precombining Versus Postcombining in Fixed Multipath

As we discussed earlier, the postcombining MMSE receiver has serious tracking problems in fast-fading channels. However, it is still interesting to compare the BER performance of the two versions of the MMSE-S-DFDs and LMMSE receivers in fixed multipath channels (no fading). The results of this investigation are shown in Figure 5.6 where we fix the SNR to 12 dB and obtain the BER performance versus the number of users. The postcombining MMSE-S-DFD and postcombining LMMSE receiver always have better performance than their precombining counterparts. More importantly, our results show that the performance difference between the nonlinear

precombining technique and its postcombining counterpart is relatively small. This is of course not the case for the LMMSE where the postcombining receiver is shown to offer much larger gain than the precombining one, especially in systems with heavy loads. Our argument here is that both precombining and postcombining MMSE-S-DFDs cancel interference from the symbols in D_k set while suppressing interference from the symbols in U_k in a MMSE sense. That is, the FBF in the MMSE-S-DFD can significantly suppress or completely cancel many effective interfering users (assuming no errors in the feedback direction). This in turn, relaxes the requirements of the FFF since it needs only to deal with small levels of signal interference. As such, the performance of the MMSE-S-DFD performs in a way similar to the LMMSE in the presence of few interfering users. In other words, the performance gap between the two versions of the nonlinear MMSE-S-DFD should be similar to that of their linear counterparts in systems with small number of users (see Figure 5.6). This result is important since one can rely on the same precombining nonlinear adaptive receiver (with minimal degradation) in channels that experience both fast and slow time variations within a block of data.

5.4.5 Convergence

Here, we examine the convergence behavior of the 2-stage precombining MMSE-S-DFD at two different system loads. These results are shown in Figure 5.7, and compared with the precombining LMMSE receiver. It is seen that the 2-stage precombining adaptive MMSE-S-DFD achieves lower steady-state MSE than its linear

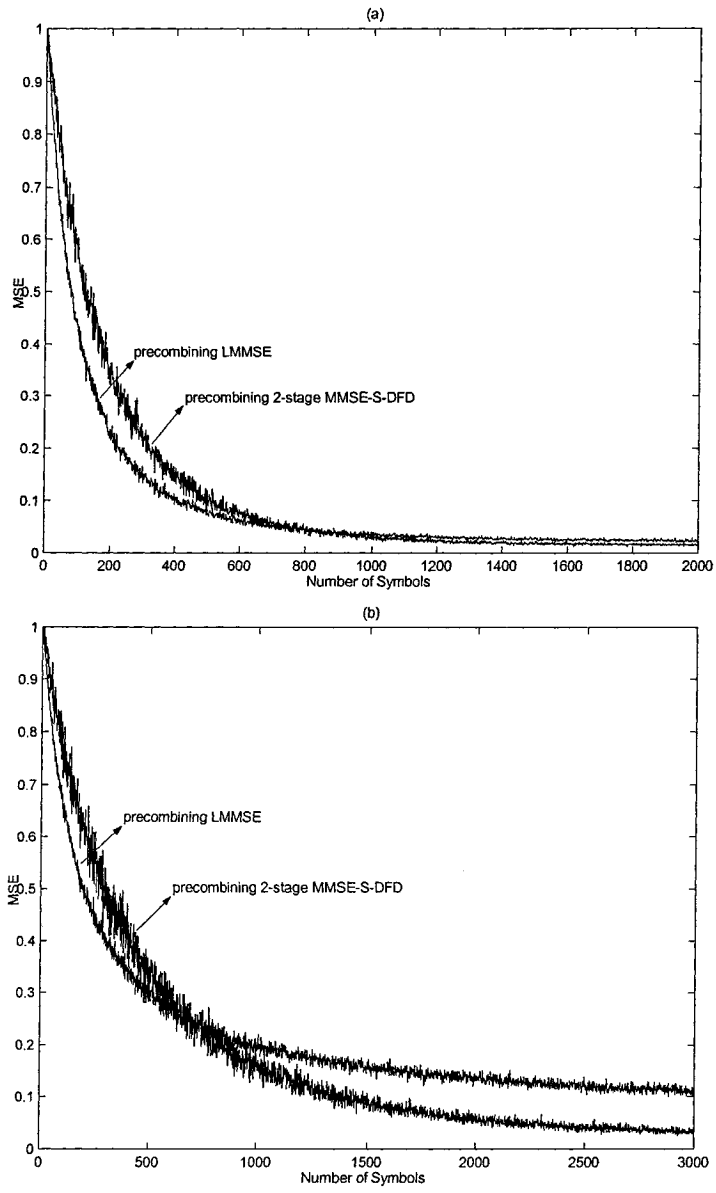

Figure 5.7: Convergence of the precombining adaptive LMMSE receiver and the 2-stage precombining adaptive MMSE-S-DFD receiver in a two-path fading channel with SNR=12 dB and 31-chip Golden codes. (a) 6 users; (b) 12 users.

counterpart in both scenarios. However, the improvement is more significant for the system with 12 users as shown in Figure 5.7.b. We noted that the linear MMSE receiver always has a faster convergence rate than the MMSE-S-DFD, especially in systems with heavy loads.

5.5 Conclusion

In this Chapter, we introduced a modified adaptive MMSE decision-feedback detection scheme for multipath fast-fading channels. The adaptive implementation of the nonlinear receiver is quite simple, yet effective in both fast and slow fading channels. Compared to the precombining LMMSE receiver, the modified precombining nonlinear receiver is shown to offer a substantial performance improvement over both slow and fast-fading channels. Most importantly, we demonstrated that the MMSE-S-FDF is robust in channels with large interference levels manifest in heavily loaded systems with large number of resolvable paths. Considering a flat fast-fading channel, and heavily loaded system, the precombining MMSE-S-DFD offers no performance degradation relative to its performance in slow fading channels. Furthermore, we have demonstrated that the precombining MMSE-S-DFD performs close to its postcombining counterpart in fixed multipath channels. Finally, we examined the convergence behavior of the adaptive nonlinear receiver and noted a slower convergence rate relative to the LMMSE in heavily loaded systems.

Chapter 6

Conclusion and Future Work

6.1 Conclusion

A brief summary of the accomplished work is presented in this section, with an emphasis on the contribution to the area of multiuser detection.

In this thesis we first proposed a new parallel interference cancellation multiuser detector based on the blind adaptive MMOE algorithm. The proposed algorithm has a computational complexity which grows linearly with the number of users. The BER performance of the proposed detector is identical to the optimum LMMSE receiver in synchronous CDMA systems. On the other hand, The proposed receivers degrade when asynchronous transmission is present, but is still within 2 dB (in SNR) of the optimum LMMSE receiver. It was also observed that the proposed adaptive MMOE-PIC detector can greatly improve the convergence speed and BER performance of the conventional adaptive MMOE receiver.

In Chapter 4, we considered a new multistage detector for frequency-selective channels. The proposed multistage detector, namely LCMV-HD-PIC detector, employs blind adaptive LCMV algorithm as the first stage followed by IC stages. The simulation results show that the proposed detector can offer an excellent tradeoff between complexity and performance. In particular, a 3-stage LCMV-HD-PIC receiver can achieve a performance which approaches that of ideal detection (single user detection) without interference and is independent of system loads and near-far problem in flat fast-fading channels. When it comes to frequency-selective fading channels, a 4-stage LCMV-HD-PIC receiver was shown to perform within 1 dB (in SNR) of the single user bound at most practical system loads and SNR's.

In Chapter 5, we presented a nonlinear MMSE decision feedback multiuser detector based on successive interference cancellation for multipath fast-fading channels. The proposed MMSE-S-DFD receiver employs a modified MMSE criterion and incorporates channel coefficients into feedback filter, and therefore can be made adaptively even in relatively fast fading channels. It was shown that the proposed nonlinear multiuser detector significantly outperforms its linear counterpart in either flat or frequency-selective fading channels. Moreover, the performance loss due to the utilization of the modified MMSE criterion instead of standard MMSE optimization function is negligible for the proposed nonlinear decision feedback detector. Finally, we considered a 2-stage MMSE-S-DFD to achieve a uniform performance over users with successive demodulation.

6.2 Future Work

Some topics for future study are now addressed. For numerical and simulation results presented in Chapter 3 and 4, we assume that the receiver has perfect knowledge of the signature waveform used to modulate the bits of the desired user. However, this may not be true in practice. In addition, as we mentioned before, the blind adaptive algorithms that we used in Chapter 3 and 4 are extremely sensitive to inaccuracies in the acquisition of the desired user's timimg and spreading code. Thus, how the proposed MMOE-PIC and LCMV-HD-PIC detectors are affected by imperfect spreading sequence estimate would be a good topic to investigate. In addition, if the performance of the proposed detectors are not satisfactory under the spreading sequence mismatch, searching for another blind adaptive algorithm which is robust to code and timing inaccuracies would be another useful topic. In this case, the blind adaptive LCCM detector [46] seems to be a good candidate since it can provide better performance than the blind adaptive MMOE receiver and is not sensitive to the errors in timing and spreading code estimates.

All of the research conducted in Chapter 3 and 4 has focused on standard ("brute force") PIC detector and no partial interference cancellation has been used for the proposed receivers. On the other hand, we noted that the proposed LCMV-HD-PIC detector shows an error floor at high SNR's due to the severe decision error propagation which can be effectively relieved by partial interference cancellation [43]. In our opinion, further work is needed to add the merit of partial interference cancellation to

the proposed receivers in this dissertation to combat error propagation. In particular, one should consider the problem of determining a good set of weights for partial PIC with only few stages.

Appendix A

Gold Sequences

Gold sequences are useful due to the large number of codes that they supply. They can be chosen so that over a set of codes available from a given generator, the cross-correlation between the codes is uniform and bounded [87, 88]. In this appendix we describe how we generate a set of Gold sequences.

Let u and v represent a preferred pair of m-sequences [87] having period $N = 2^n - 1$. The family of codes defined by $\{u, u+v, u+Dv, u+D^2v, ..., u+D^{N-1}v\}$, where D is the delay element, is called the set of Gold codes for this preferred pair of m-sequences [25]. It can be proved that the $N+1$ elements of Gold codes set have the property that the cross-correlation between any pair of codes in the set is three-valued [89], where those three values are $-t(n)$, -1, and $t(n)-2$, where

$$t(n) = \begin{cases} 1 + 2^{\frac{n+1}{2}} & \text{for } n \text{ odd} \\ 1 + 2^{\frac{n+1}{2}} & \text{for } n \text{ even} \end{cases} \tag{A.1}$$

[89], where those three values are $-t(n)$, -1, and $t(n)-2$, where

$$t(n) = \begin{cases} 1+2^{\frac{n+1}{2}} & \text{for } n \text{ odd} \\ 1+2^{\frac{n+1}{2}} & \text{for } n \text{ even} \end{cases} \tag{A.1}$$

A set of Gold codes with length 31 is generated by two preferred m-sequences with generator polynomials which are described by the parity polynomials

$$\begin{aligned} h_1(p) &= p^5+p^2+1 \\ h_2(p) &= p^5+p^4+p^2+p+1 \end{aligned}$$

The registers for generating the two m-sequences and the corresponding Gold sequences are shown in Figure A.1. In this case, there are 33 different sequences corresponding to the 33 relative phases of the two m-sequences. We choose a subset of codes from the set of 33 codes so that the cross-correlation between each pair is -1. The autocorrelation of each code is obviously 31, i.e equal to the length of the code.

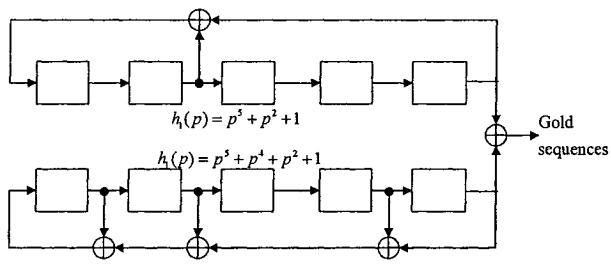

Figure A.1: Generation of Gold sequences of length 31

Appendix B

List of Abbreviations

AWGN	additive white Gaussian noise
BER	bit error rate
BPSK	binary phase-shift keying
DS-CDMA	direct sequence code division multiple access
DFD	decision feedback detection
FDMA	frequency division multiple access
GSC	generalized sidelobe canceller
HD	hard decision
LCCM	linear constrained constant modulus
LCMV	linear constrained minimum variance
LMMSE	linear minimum mean-squared-error
LMS	least mean square
MAI	multiple access interference
MAP	maximum-a-posteriori
MLS	maximum likelihood sequence
MMOE	minimum mean-output-energy
MUD	multiuser detection
PIC	parallel interference cancellation
SD	soft decision
SIC	successive interference cancellation
SIR	signal to interference ratio
SNR	signal to noise ratio
SSMA	spread spectrum multiple-access
TDMA	time division multiple access

Table B.1: List of Abbreviations

Bibliography

[1] A. J. Viterbi, "Wireless digital communications: A view based on three lessons learned," IEEE Communications Magazine, pp. 33-36, Sept. 1991.

[2] R. Pickholtz, D. Schilling, L. Milstein, "Theory of spread-spectrum communications - A tutorial," IEEE Trans. Commmunications, pp. 855-884, May. 1982.

[3] QUALCOMM, Inc., Proposed EIA/TIA Interim Standard, Apr. 1992.

[4] U. C. Fiebig et al, "Design study for a CDMA-based third generation mobile radio system," IEEE Journal on Selected Areas in Communications, vol. 12, pp. 733-743, May. 1994.

[5] F. Adachi et al, "Coherent multicode DS-CDMA mobile radio access," IEICE Tans. communications, vol. E79-B, pp. 1316-1325, Sept. 1996.

[6] E. Dahlman, B. Gudmundson, and J. Sköld, "UMTS/IMT-2000 based on wideband CDMA," IEEE Communications Magazine, vol. 36, pp. 70-80, Sept. 1998.

[7] T. Ojanperä and R. Prasad, "An overview of air interface multiple access for IMT-2000/UMTS," IEEE Communications Magazine, vol. 36, pp. 82-95, Sept. 1998.

[8] F. Adachi, M. Sawahashi, and H. Suda, "Wideband DS-CDMA for next generation mobile communications systems," IEEE Communications Magazine, vol. 36, pp. 56-69, Sept. 1998.

[9] Y. Ishida, "Recent study on candidate radio transmission technology for MIT-2000," in 1st Annual CDMA Eyro. Cong., Oct. 1997.

[10] S. Verdú, "Minimum probability of error for asynchronous Gaussian multiple-access channels," IEEE Trans. Inform. Theory, vol. 32, pp. 85–96, Jan. 1986.

[11] S. Verdú, "Optimum multiuser asymptotic efficiency," IEEE Trans. Commun., vol. 34, pp. 890–897, Sept. 1986.

[12] R. Lupas and S. Verdú, "Near–far resistance of multiuser detectors in asynchronous channels," IEEE Trans. Commun., vol. 38, pp. 496–508, Apr. 1990.

[13] R. Lupas and S. Verdú, "Linear multiuser detectors for synchronous code-division multiple-access channels," IEEE Trans. Inform. Theory, vol. 35, pp. 123–136, Jan. 1989.

[14] M. K. Varanasi and B. Aazhang, "Multistage detection in asynchronous code-division multiple-access communications," IEEE Trans. Commun., vol. 38, pp. 509–519, Apr. 1990.

[15] M. K. Varanasi and B. Aazhang,"Near-optimum detection in synchronous code-division multiple-access systems," IEEE Trans. Commun., vol. 39, pp. 725–736, May 1991.

[16] A. Duel-Hallen, "Decorrelating decision feedback multiuser detector for synchronous code-division multiple-access channel," IEEE Trans. Commun., vol. 41, pp. 285–290, Feb. 1993.

[17] A. Duel-Hallen, "A family of decision feedback multiuser detetcors for asynchronous code-division multiple-access channels," IEEE Trans. Commun., vol. 43, nos. 2/3/4, pp. 421–434, 1995.

[18] Z. Xie, C. T. Rushforth, and R. T. Short, "Multi-user signal detection using sequential decoding," IEEE Trans. Commun., vol. 38, pp. 578–583, May 1990.

[19] Z. Xie, R. T. Short, and C. T. Rushforth, "A family of suboptimum detectors for coherent multiuser communications," IEEE J. Select. Areas Commun., vol. 8, pp. 683–690, May 1990.

[20] K. Schneider, "Optimum detection of code division multiplexed signals," IEEE Trans. Aerospace and Electronic Systems, vol. AES-15, pp. 181-185, Jan. 1979.

[21] K. Schneider, "Crosstalk resistance receiver for M-ary multiplexed communications," IEEE Trans. Aerospace and Electronic Systems, vol. AES-16, pp. 426-433, July. 1980.

[22] R. Kohno, H. Imai, and M. Hatori, "Optimum receiver using canceller of co-channel interference in SSMA," in 1982 IECE National Conf. (Spring), 1982, pp. 197-201, In Japanese.

[23] R. Kohno, H. Imai, and M. Hatori, "Cncellation techniques of co-channel interference and application of viterbi algorithm in asynchronous spread spectrum multiplex access systems," in Proc. 1982 Symp. on Information Theory and Its Applications, Oct. 1982, pp. 659-666, In Japanese.

[24] R. Kohno, H. Imai, and M. Hatori, "Cancellation techniques of co-channel interference in asynchronous spread spectrum multiplex access systems," Electronics and Communications, vol. 66-A, pp. 20-29, 1983.

[25] J. G. Proakis, Digital Communications, 2nd ed, New York: Mcgraw-Hill, 1989.

[26] S. Verdú, Multiuser Detection, Cambridge University Press, 1998.

[27] S. Verdú, "Minimum probability of error for asynchronous multiple-access communications systems," in Proc. 1983 IEEE Military Communications Conf., Mov. 1983, vol. 1, pp. 213-219.

[28] R. Iltis and L. Mailaender, "Multiuser detection of quasi-synchronous CDMA signals using linear decorrelators," IEEE Trans. Commun., vol. 44, pp. 1561–1571, Nov. 1996.

[29] M. Tsatsanis, "Inverse filtering criteria for CDMA systems," IEEE Trans. Signal Processing, vol. 45, pp. 102–112, Jan. 1997.

[30] M. Juntti and B. Aazhang, "Finite memory-length linear multiuser detection for asynchronous CDMA communications," IEEE Trans. Commun., vol. 45, pp. 611–622, May 1997.

[31] X. Wang and H. V. Poor, "Blind multiuser detection: A subspace approach," IEEE Trans. Inform. Theory, vol. 44, pp. 91–103, Jan. 1998.

[32] M. K. Varanasi and B. Aazhang, "Optimally near–far resistant multiuser detection in differentially coherent synchronous channels," IEEE Trans. Inform. Theory, vol. I37, pp. 1006–1018, July 1991.

[33] J. Yang and S. Roy, "On joint transmitter and receiver optimization for multiple-input–multiple-output (MIMO) transmission," IEEE Trans. Commun., vol. 42, Dec. 1994.

[34] U. Madhow and M. L. Honig, "MMSE interference suppression for direct-sequence spread-spectrum CDMA," IEEE Trans. Commun., vol. 32, pp. 3178–3188, Dec. 1994.

[35] H. V. Poor and S. Verdú, "Probability of error in MMSE multiuser detection," IEEE Trans. Inform. Theory, vol. 43, pp. 858–871, May 1997.

[36] S. L. Miller, "An adaptive direct-sequence code-division multiple-access receiver for multiuser interference rejection," IEEE Trans. Commun., vol. 43, pp. 1746–1755, Feb./Mar./Apr. 1995.

[37] P. B. Rapajic and B. S. Vucetic, "Adaptive Receiver Structures for Asynchronous CDMA Systems," IEEE J. Select. Areas Commun., vol. 12, PP. 685-697, May. 1994.

[38] S. Verdú, "Adaptive multiuser detection," in Proc. IEEE Int. Symp. on Spread Spectrum Theory and Applications (Oulu, Finland, July 1994).

[39] A. J. Viterbi, "Very low rate convolution codes for maximum theoretical performance of spread-spectrum multiple-access channels," IEEE JSAC, vol. 8, no. 4, May 1990, pp. 641-649.

[40] R. Kohno et al., "Combination of an adaptive array antenna and a canceller of interference for direct-sequence code-division multiple-access system," IEEE JSAC, vol. 8, no. 4, May 1990, pp. 675-682.

[41] S. Moshavi, "Multistage linear detectors for DS-CDMA communications," Ph. D dissertatation, Dept. Elec. Eng., City Univ. New York, NY, Jan. 1996.

[42] R. M. Buehrer and B. D. Woerner, "Analysis of adaptive multistage interference cancellation for CDMA using an improved Gaussian approximation," Proc. IEEE MILCOM '95, San Diego, CA, Nov. 1995, pp. 1195-1199.

[43] D. Divsalar, M. K. Simon, and D. Raphaeli, "Improved parallel interference cancellation for CDMA," IEEE Trans. Commun., vol. 46, pp. 258-268, Feb. 1998.

[44] M. Honig, U. Madhow, and S. Verdú, "Blind adaptive multiuser detection," IEEE Trans. Inform. Theory, vol. 41, pp. 944–960, July 1995.

[45] M. K. Tsatsanis and Z. Xu, "Performance analysis of minimum variance CDMA receivers," IEEE Trans. Signal Processing, vol. 46, pp. 3014–3022, Nov. 1998.

[46] J. Míguez and L. Castedo, "A linearly constrained constant modulus approach to blind adaptive multiuser interference suppression," IEEE Communications Letters, vol. 2, pp. 217-219, Aug. 1998.

[47] Zhengyuan Xu and Ping Liu, "Blind Multiuser Detection by Kurtosis Maximization/Minimization," IEEE Trans. Signal Processing, vol. 11, pp. 1-4, Jan. 2004.

[48] Anders Høst-Madsen and Kyung-Sean Cho, "MMSE/PIC Multiuser Detection for DS/CDMA Systems with Inter- and Intra-Cell Interference," IEEE Trans. Commun., vol. 47, pp. 291-299, Feb. 1999.

[49] Simon Haykin, Adaptive Filter Theory, Englewood Cliffs, NJ: Prentice Hall, 1986.

[50] Dongning Guo, Lars K. Rasmussen, Sumei Sun and Teng J. Lim, "A Matrix-Algebraic Approach to Linear Parallel Interference Cancellation in CDMA," IEEE Trans. Commun., vol. 48, pp. 152-161, Jan. 2000.

[51] Z. Zvonar and D. Brady, "Multiuser detection in single-path fading channels," IEEE Trans. Commun., vol. 42, pp. 1729–1739, Feb./Mar./Apr. 1994.

[52] Z. Zvonar, "Multiuser detection for Rayleigh fading channels," Ph.D. dissertation, Northeastern Univ., Boston, MA, Sept. 1993.

[53] Z. Zvonar, "Multiuser detection in asynchronous CDMA frequency-selective fading channels," Wireless Personal Commun., vol. 3, no. 3–4, pp. 373–392, 1996.

[54] M. K. Varanasi, "Parallel group detection for synchronous CDMA communication over frequency-selective Rayleigh fading channels," IEEE Trans. Inform. Theory, vol. 42, pp. 116–128, Jan. 1996.

[55] M. K. Varanasi and S. Vasudevan, "Multiuser detectors for synchronous CDMA communication over nonselective Rician fading channels," IEEE Trans. Commun., vol. 42, pp. 711–722, Feb./Mar./Apr. 1994.

[56] S. Vasudevan and M. K. Varanasi, "Optimum diversity combiner based multiuser detection for time-dispersive Ricean fading CDMAchannels," IEEE J. Select. Areas Commun., vol. 12, pp. 580–592, May 1994.

[57] A. Klein and P. W. Baier, "Linear unbiased data estimation in mobile radio systems applying CDMA," IEEE J. Select. Areas Commun., vol. 11, pp. 1058–1066, Sept. 1993.

[58] Z. Zvonar and D. Brady, "Suboptimal multiuser detector for frequencyselective Rayleigh fading synchronous CDMA channels," IEEE Trans. Commun., vol. 43, pp. 154–157, Feb./Mar./Apr. 1995.

[59] M. Stojanovic and Z. Zvonar, "Performance of linear multiuser detectors in time-varying multipath fading CDMA channels," in Proc. Commun. Theory Mini-Conf. in Conjunction with IEEE Global Telecommun. Conf., London, U.K., Nov. 18–22, 1996, pp. 163–167.

[60] S. L. Miller and A. N. Barbosa, "A modified MMSE receiver for detection of DS-CDMA signals in fading channels," in Proc. 1996 IEEE Military Communications Conf., pp. 898–902.

[61] A. N. Barbosa and S. L. Miller, "Adaptive detection of DS-CDMA signals in fading channels," IEEE Trans. Commun., vol. 46, pp. 115–124, Jan. 1998.

[62] M. Honig, M. Shensa, S. L. Miller, and L. B. Milstein, "Performance of adaptive linear interference suppression for DS-CDMA in the presence of flat Rayleigh fading," in Proc. 1997 IEEE Vehicular Technology Conf., 1997.

[63] H. C. Huang and S. Verdú, "Linear differentially coherent multiuser detection for multipath channels," Wireless Pers. Commun., vol. 6, no. 1/2, pp. 113–136, 1998.

[64] X. Wang and H. V. Poor, "Blind equalization and multiuser detection in dispersive CDMA channels," IEEE Trans. Commun., vol. 46, pp. 91–103, Jan. 1998.

[65] M. Latva-aho, "Advanced receivers for widebandCDMAsystems," Faculty of Technol., Univ. of Oulu, 1998.

[66] U. Fawer and B. Aazhang, "A multiuser receiver for code division multiple access communications over multipath channels," IEEE Trans. Commun., vol. 43, pp. 1556–1565, Feb./Mar./Apr. 1995.

[67] P. Patel and J. Holtzman, "Analysis of a simple successive interference cancellation scheme in a DS/CDMA system," IEEE J. Select. Areas Commun., vol. 12, pp. 796–807, June 1994.

[68] A. Hottinen, H. Holma, and A. Toskala, "Performance of multistage multiuser detection in a fading multipath channel," in IEEE Proc. Int. Symp. Personal, Indoor and Mobile Radio Commun., vol. 3, Toronto, Canada, Sept. 27–29, 1995, pp. 960–964.

[69] M. Latva-aho and J. Lilleberg, "Parallel interference cancellation in multiuser CDMA channel estimation," Wireless Personal Commun., vol. 7, pp. 171–195, Aug. 1998.

[70] U. Fawer and B. Aazhang, "Multiuser receivers for code-division multiple-access systems with trellis-based modulation," IEEE Journal on Selected Areas in Communications., vol. 14, pp. 1602–1609, Oct. 1996.

[71] J. D. Parsons, The Mobile Radio Propagation Channel, London, U.K.: Pentech, 1992.

[72] B. D. Van. Veen and K. M. Buckley, "Beamforming: a versatile approach to spatial filtering," IEEE ASSP Mag., pp. 4-24, Apr. 1988.

[73] M. J. Juntti and J. O. Lilleberg, "Implementation aspects of linear multiuser detectors in asynchronous CDMA systems," in IEEE Proc. Int., Symp. Spread

Spectrum Techniques and Applications, vol. 2, Mainz, Germany, Sept. 22–25, 1996, pp. 842–846.

[74] M. J. Juntti, "Linear multiuser detector update in synchronous dynamic CDMA systems," in IEEE Proc. Int. Symp. Personal, Indoor and Mobile Radio Commun., vol. 3, Toronto, Canada, Sept. 27–29, 1995, pp. 980–984.

[75] William C. Jake, Microwave mobile Communications, IEEE Press, 1994.

[76] M. J. Juntti, B. Aazhang, and J. O. Lilleberg, "Iterative implementation of linear multiuser detection for dynamic asynchronous CDMA systems, " IEEE Trans. Commun., vol. 46, Issue:4, pp. 503-508, April 1998.

[77] M. Latva-aho and M. J. Juntti, "MMSE detection of DS-CDMA systems in fading channels," IEEE Trans. Commun., vol. 48, pp. 194–199, Feb. 2000.

[78] S. L. Miller, M. Honig, and L. B. Milstein, "Performance analysis of MMSE receivers for DS-CDMA in frequency-selective fading channels," IEEE Trans. Commun., vol. 48, pp. 1919-1929, Nov. 2000.

[79] M. Honig, S. Miller, M. Shensa, and L. Milstein, "Performance of adaptive linear interference suppression in the presence of dynamic fading," IEEE Trans. Commun., vol. 49, pp. 635–645, Apr. 2001.

[80] H. Dai and H. V. Poor, "Sample-by-sample adaptive space-time processing for multiuser detection in multipath CDMA systems," in Proc. Fall IEEE Vehicular Technology Conf., Atlantic City, NJ, Oct. 7-11, 2001.

[81] G. Woodward, M. L. Honig, P. B. Rapajic and R. Ratasuk, "Minimum mean-squared-error multiuser decision-feedback detectors for DS-CDMA," IEEE Trans. Commun., vol. 50, pp. 2104- 2112, Dec. 2002.

[82] R. Ratasuk, G. Woodward, and M. L. Honig, "Adaptive multiuser decision feedback for asynchronous cellular DS-CDMA," in Annu. Allerton Conf. Communications, Control and Computing, Monticello, IL, Sept. 1999, pp. 1236–1245.

[83] P. B. Rapajic and B. S. Vucetic, "Adaptive Receiver Structures for Asynchronous CDMA Systems," IEEE J. Select. Areas Commun., vol. 12, PP. 685-697, May. 1994.

[84] J. E. Smee and S. C. Schwartz, "Adaptive space-time feed-forward/feedback detection for high data rate CDMA in frequency-selective fading," IEEE Trans. Commun., vol. 49, pp. 317-328, Feb. 2001.

[85] M. L. Honig, G. Woodward, and Y. Sun, "Adaptive iterative multiuser decision feedback detection," IEEE Trans. on Wireless Commun., vol. 3, pp. 477- 485, Mar. 2004.

[86] P. Fan and M. Darnell, Sequence Design for the Communication Application, Research Studies Press, U.K., 1996.

[87] R. Gold, "Optimal binary sequences for spread spectrum multiplexing," IEEE Trans. Information Theory, vol. 14, pp. 619-621, Oct. 1967.

[88] R. Gold, "Maximal recursive sequences with 3-valued recursive cross-correlation functions," IEEE Trans. Information Theory, vol. 4, pp. 154-156, Jan. 1968.

[89] M. K. Varanasi, "Decision Feedback Multiuser Detection: A Systematic Approach," IEEE Trans. Information Theory, vol. 45, pp. 219-240, Jan. 1999.

[90] M. L. Honig and H. V. Poor, "Adaptive interference mitigating in wireless communications systems," in Wireless Communications: A Signal Processing Perspective, H. V. Poor and G. Wornell, Eds. Englewood Cliffs, NJ: Prentice-Hall, 1998.

[91] G. H. Golub and C. F. Van Loan, Matrix Computations, 2nd ed. Baltimore, MD: Johns Hopkins Univ. Press, 1989.